

Universidade de Lisboa  
Faculdade de Ciências  
Departamento de Biologia Animal



**Optimization of the differentiation process of umbilical cord  
matrix mesenchymal stem cells into hepatocyte-like cells**

**Alexandra Martins de Medeiros Vieira da Silva**

Dissertação  
Mestrado em Biologia Evolutiva e do Desenvolvimento

**2013**

Universidade de Lisboa  
Faculdade de Ciências  
Departamento de Biologia Animal



**Optimization of the differentiation process of umbilical cord  
matrix mesenchymal stem cells into hepatocyte-like cells**

**Alexandra Martins de Medeiros Vieira da Silva**

Dissertação

Mestrado em Biologia Evolutiva e do Desenvolvimento

Dissertação orientada por:

Doutora Joana Miranda - iMed-FFUL

Professora Doutora Gabriela Rodrigues - FCUL

**2013**

## Acknowledgements

First of all I would like to thank the team CBT-iMED for receiving me and for making this thesis project possible.

To my supervisor at CBT-iMED, Dra. Joana Miranda, I would like to express my sincere gratitude for her patience in guiding me during all the process of research and writing. To Professora Gabriela Rodrigues, my FCUL supervisor, for being always available for receiving me and help.

I would also like to thank to my colleagues at CBT-iMED laboratory, in no particular order: Elysse Filipe, Patrícia Guerreiro, Pedro Pinheiro, Madalena Cipriano, Sérgio Camões, João Costa, Ana Matos, Sandrina Gonçalves and Nuno Torres. Thank you for your help, with your sense of humour and positivity you always made my day better.

I also thank Prof. Nuno Oliveira, Prof. Fátima Cabral, Prof. Judite Costa, and Prof. Ana Francisca for their advice and suggestions.

To my friends: Fábio, Daniela, Filipe, Catarina, Clara, Maié, Mário, Sara Mendes, Sara Costa, Ana Quendera, Ana Marques, Gonçalo, António, Cláudia and Renato for their support.

To my parents, my sister, my family in Azores and Jorge who are always by my side.

## Abstract

The few literature described protocols of hepatic differentiation of human umbilical cord matrix mesenchymal stem cells (ucmMSC) lead to populations of cells with less than satisfactory differentiation rates.

In this study a hepatic differentiation protocol was firstly optimized in conventional monolayer (2D) cultures and further implemented in a 3D culture method, in order to achieve a homogenous population of functional hepatocyte-like cells (HLCs), as part of the creation of an alternative model for *in vitro* toxicology studies.

UCX<sup>®</sup>, ucmMSC isolated by a proprietary method developed by ECBio S.A., were subjected to 4 differentiation protocols in 2D culture conditions being the most promising procedure applied to 3D culture method. The characterization of differentiated UCX<sup>®</sup> included the analysis of the expression of hepatic markers by quantitative real time reverse-transcription polymerase chain reaction (qRT-PCR) and immunofluorescence assays. Metabolic activity was assessed through ECOD and UGT activity assay, and also by glycogen accumulation and urea production. Undifferentiated UCX<sup>®</sup>, HepG2 and primary rat hepatocytes were used as controls.

The HLCs that resulted from the optimized protocol showed hepatocyte-like morphology, expression of hepatic lineage markers, including ALB, CK18 and HNF4 $\alpha$  as well as the underexpression of CK19. These also exhibited biotransformation activity (ECOD and UGT activities), and the ability to store glycogen and to produce urea.

When transposed into 3D cultures, the optimized method induced the expression of hepatic markers CK18, HNF4 $\alpha$  and ALB and higher urea production.

In summary a more homogenous and functional population of HLCs, with hepatocyte expression pattern and metabolic activity at a superior level than HepG2 and in some aspects at the same activity level of rat primary hepatocytes, was successfully obtained, opening doors to the construction of a humanly-close metabolism and toxicology model for drug testing.



## Keywords

Differentiation, Hepatocytes, Mesenchymal stem cells (MSCs), Umbilical Cord matrix, UCX®, toxicology model.

## Resumo

O fígado é o maior órgão interno do corpo humano, sendo este constituído por células parenquimatosas e não parenquimatosas. No grupo das células parenquimatosas, incluem-se os hepatócitos, que constituem 60% a 70% do número total de células do fígado. As células endoteliais, células de Kupffer, células de Ito e células estaminais (células ovais) são as células não parenquimatosas do fígado [1-2].

O fígado desempenha funções muito importantes no organismo, nomeadamente, o armazenamento e processamento dos nutrientes, produção de proteínas plasmáticas e destoxificação do organismo através da alteração da estrutura de moléculas ou através da excreção pela bília [2]. O ciclo da ureia é o principal processo de destoxificação do sangue, responsável pela conversão de amónia em ureia, sendo esta depois filtrada e excretada pelos rins [2].

O fígado é também o principal órgão responsável pela biotransformação. Os hepatócitos expressam enzimas de biotransformação de fase I e fase II: os citocromos P450, enzimas de fase I responsáveis pelas vias de oxidação, redução e hidrólise que adicionam ou expõem um grupo funcional, como hidroxilo, tiol, ou amina ao substrato. As reações de fase II conduzem à formação de conjugados desses mesmos grupos funcionais com ácido glucurónico, sulfato e glutatona, que levam à eliminação directa (no caso dos dois primeiros) e destoxificação (no caso da conjugação com glutatona) das moléculas metabolizadas [3].

Sendo o fígado o principal órgão de metabolização de xenobióticos, este é mais exposto aos efeitos potencialmente tóxicos dos fármacos e seus metabolitos. Para detectar precocemente os potenciais riscos toxicológicos é essencial ter bons modelos *in vitro* de teste de fármacos antes de estes entrarem em ensaios clínicos [4].

Vários modelos *in vitro* são usados em estudos de toxicologia, por exemplo: bactérias ou vírus modificados geneticamente para expressarem isoformas de enzimas de fase I e fase II [5-6], fígados isolados [1, 7], culturas primárias de hepatócitos [1, 8] e linhas celulares [9-10].

Modelos baseados na perfusão do fígado, tanto *in vivo* com *ex vivo*, são muito utilizados para testar o metabolismo hepático e farmacocinética. Estes modelos têm a capacidade de manter a estrutura hepática intacta, todavia a complexidade do mesmo dificulta a compreensão dos processos que ocorrem a nível intracelular [1, 7].

Os modelos celulares mais utilizados baseiam-se em linhas celulares de carcinoma hepatocelular, como HepG2 e HepRG [9-10]. HepG2 é uma linha celular humana acessível, fácil de manter em cultura. Todavia, não apresenta algumas funções características dos hepatócitos, como por exemplo, apresenta um perfil de expressão de enzimas de biotransformação diferente [10]. Recentemente, foi isolada e caracterizada a linha celular-HepRG. Estas células encontram-se num estado bipotente semelhante ao de hepatoblasto e a sua maturação pode ser induzida através da adição de 2% dimetil sulfóxido (DMSO) e 50  $\mu$ M hidrocortisona. Quando maturadas, estas células expressam 85% dos genes expressos em hepatócitos humanos. Contudo, muitos marcadores importantes não são expressos, como é o caso dos factores de transcrição C/EBP $\alpha$ , C/EBP $\beta$  e enzimas de fase II [9].

Os hepatócitos primários, são um modelo de excelência para a compreensão de processos metabólicos e efeitos hepatotóxicos de fármacos [1, 11], dado que durante um período de tempo após o seu isolamento, preservam muitas das funções hepáticas, como a capacidade de biotransformação, metabolismo de glucose e destoxificação da amónia. Apesar disso, a dificuldade em obter material biológico traduz-se na difícil implementação deste sistema de forma contínua e prolongada [1].

O uso de hepatócitos primários de rato é mais acessível, porém existem diferenças interespecies que não permitem a total correlação entre este modelo e o fígado

humano *in vivo*. Além de que, a perda de funcionalidade persiste, problema inerente a todos os hepatócitos primários [12-13].

Tendo em consideração os problemas éticos e diferenças interespecies mencionados, um novo método foi proposto como alternativa para substituir as culturas de hepatócitos primários nos ensaios de toxicologia, que se baseia na utilização de hepatócitos obtidos por diferenciação de células estaminais humanas [1, 4, 14].

Os protocolos de diferenciação em hepatócitos são alicerçados nos 4 passos do desenvolvimento do fígado: indução da formação da endoderme, indução da competência hepática, formação de hepatoblastos e finalmente maturação em hepatócitos [15].

Como ponto de partida para esta diferenciação já foram testados diferentes tipos de células: células estaminais embrionárias [16-19], células mesenquimais da medula óssea [20-21], adipócitos [22], e células estaminais pluripotentes induzidas [23-24]. Todavia os estudos que utilizam células estaminais mesenquimais do cordão umbilical para esta finalidade, são escassos [25]. O cordão umbilical é uma fonte muito vantajosa de células estaminais mesenquimais visto que permite um isolamento inicial rápido de um grande número de células multipotentes e a sua utilização levanta muito menos problemas éticos [26-27].

Os sistemas de cultura em monocamada (2D) são muito utilizados para a cultura *in vitro* de hepatócitos. Este tipo de cultura obriga os hepatócitos a adquirirem uma morfologia achatada que não corresponde à que possuem no ambiente *in vivo* [1-2]. Recentemente, têm-se vindo a abordar modelos de cultura em 3D. São vários os métodos que se podem aplicar, entre os quais se destaca o método de formação de agregados [28]. Esta técnica assenta sobre a capacidade inata que algumas células têm em se agregar, permitindo a formação de matriz extracelular natural, de extrema importância na manutenção das funções dos hepatócitos [1].

Neste sentido, o objectivo deste trabalho foi desenvolver um protocolo para diferenciação de células mesenquimais estaminais da matriz do cordão umbilical (UCX®) em hepatócitos maduros com a finalidade de se criarem modelos de toxicologia.

Com o intuito de se obter uma população homogénea e funcional de hepatócitos, algo não alcançado em estudos anteriores, novos protocolos foram testados e implementados em modelos 3D que permitem reproduzir melhor o ambiente *in vivo*, logo, tendo um grande potencial para aumentar o sucesso da diferenciação em hepatócitos.

Nas UCX® diferenciadas foi analisada a expressão de marcadores hepáticos CK18, ALB e HNF4α por qRT-PCR e imunofluorescência. A atividade de biotransformação foi determinada através dos ensaios de atividade ECOD e UGT. Também foi avaliada a capacidade de acumulação do glicogénio através do método PAS e a capacidade de destoxificação da amónia, foi determinada a partir da quantificação da ureia produzida. HepG2 e hepatócitos primários de rato foram usados como controlo.

Primeiramente, foi implementado o protocolo descrito por Campard *et al.* (2008), uma vez que este foi aplicado a MSCs da matriz do cordão, para o nosso conhecimento o único. Utilizando este protocolo como base, modificações foram feitas nos 3 passos que o constituem. O protocolo optimizado permitiu a obtenção de hepatócitos com expressão dos marcadores hepáticos CK18, HNF4α e ALB com níveis de função superiores a HepG2 e em alguns ensaios ao mesmo nível que os hepatócitos primários de rato.

O protocolo optimizado em 2D foi testado em 3D, na medida em que este método permite que as células adquiram uma estrutura mais semelhante ao que acontece *in vivo* e os hepatócitos diferenciados foram caracterizados no que respeita a morfologia, através de coloração com hematoxilina eosina, detecção de marcadores hepáticos CK18, HNF4α e ALB através de imunofluorescência, acumulação de glicogénio através de coloração PAS e produção de ureia. Os resultados obtidos demonstram uma clara melhoria em termos de presença dos marcadores hepáticos (CK18, HNF4α e ALB) relativamente às células diferenciadas em 2D com o mesmo protocolo. Em relação à

atividade metabólica, as células diferenciadas em cultura 3D, apresentam maior competência em termos de metabolismo de glucose (PAS) e destoxificação de amónia, o que confirma o potencial das culturas em 3D no que respeita à diferenciação e obtenção de hepatócitos funcionais.

### Palavras-chave

Diferenciação, Hepatócitos, Células mesenquimais estaminais, Matriz do cordão umbilical, UCX<sup>®</sup>, modelos toxicológicos.

# Index

Acknowledgments	i
Abstract	ii
Keywords	iii
Resumo	iii
Palavras-chave	vii
Figure index	ix
Glossary	x
1. Introduction	1
1.1. Liver	1
1.2. <i>In vitro</i> toxicology models	2
1.2.1. 3D models	4
1.3. Alternative models	6
1.4. Objectives	13
2. Materials and methods	14
2.1. Cell culture reagents	14
2.2. Collagen extraction and plate coating	14
2.3. Cell culture	15
2.4. BCA protein quantification	15
2.5. Hepatocyte differentiation protocols	16
2.6. Quantitative real time polymerase chain reaction (qRT-PCR)	17
2.7. Immunofluorescence	18
2.8. Periodic acid Schiff's staining (PAS)	19
2.9. Hematoxylin-eosin staining (H&E)	19
2.10. Urea production	20
2.11. 7-ethoxycoumarin-O-deethylase (ECOD) activity	20
2.12. Uridine 5'-diphosphate glucuronosyltransferase (UGT) activity	21
2.13. Statistical analysis	21
3. Results	22
3.1. UCX® differentiation into hepatocyte-like cells under 2D conditions	22
3.1.1. Optimization of coating, seeding density and FBS concentration	23
3.1.2. Induction of hepatic competence	23
3.1.3. Characterization of differentiation Pattern of UCX® into hepatocyte-like cells: <i>Reference Protocol</i> , Protocol A, Protocol B and Protocol C	24 25
3.2. UCX® differentiation into Hepatocyte-like cells under 3D conditions	35
3.2.1. Characterization of the Differentiation Pattern of UCX® into hepatocyte-like Cells (HLCs): <i>Reference Protocol</i> versus Protocol C	40 45
4. Discussion	
5. Bibliography	
Annex 1	
Annex 2	

## Figure Index

Figure 1	Morphology of differentiated UCX <sup>®</sup> resultant from <i>Reference Protocol</i> with different plate coatings and FBS concentrations.	24
Figure 2	Relative <i>hhex</i> gene expression of differentiated UCX <sup>®</sup> from <i>Reference Protocol</i> and Protocol A, at day 2, of undifferentiated UCX <sup>®</sup> and HepG2, determined by qRT-PCR.	25
Figure 3	Morphology of differentiated UCX <sup>®</sup> at days 15, 21 and 24 and of undifferentiated UCX <sup>®</sup> , HepG2, and ratPHep in 2D culture method.	26
Figure 4	Relative <i>ck19</i> gene expression of differentiated UCX <sup>®</sup> resultant from <i>Reference Protocol</i> , Protocol B and C at day 24 and of undifferentiated UCX <sup>®</sup> and HepG2, determined by qRT-PCR.	27
Figure 5	Relative <i>alb</i> and <i>ck18</i> gene expression of differentiated UCX <sup>®</sup> resultant from <i>Reference Protocol</i> , Protocol B and C at day 24 and of undifferentiated UCX <sup>®</sup> and HepG2, determined by qRT-PCR.	28
Figure 6	Presence of CK18 in the differentiated UCX <sup>®</sup> at day 24, in undifferentiated UCX <sup>®</sup> , ratPHep and HepG2 in 2D culture method, detected by immunofluorescence staining.	29
Figure 7	Presence of ALB in differentiated UCX <sup>®</sup> at day 24, in undifferentiated UCX <sup>®</sup> , ratPHep and HepG2 in 2D culture method, detected by immunofluorescence staining.	30
Figure 8	Presence of HNF4 $\alpha$ in the differentiated UCX <sup>®</sup> at day 24, in undifferentiated UCX <sup>®</sup> , ratPHep and HepG2 in 2D culture method, detected by immunofluorescence staining.	31
Figure 9	ECOD activity of differentiated UCX <sup>®</sup> of differentiated UCX <sup>®</sup> at day 24 and of undifferentiated UCX <sup>®</sup> , HepG2, and ratPHep in 2D culture method.	32
Figure 10	UGT activity of differentiated UCX <sup>®</sup> at day 24 and of undifferentiated UCX <sup>®</sup> , HepG2 and ratPHep in 2D culture method.	33
Figure 11	Urea production of differentiated UCX <sup>®</sup> at day 24 and of undifferentiated UCX <sup>®</sup> , and in HepG2 and ratPHep in 2D culture method.	33
Figure 12	Glycogen accumulation in differentiated UCX <sup>®</sup> at day 24, undifferentiated UCX <sup>®</sup> , HepG2 and ratPHep in 2D culture method, revealed by PAS staining.	34
Figure 13	Undifferentiated UCX <sup>®</sup> spheroids at day 2 and differentiated UCX <sup>®</sup> spheroids of <i>Reference Protocol</i> and Protocol C at day 24.	36
Figure 14	Hematoxylin-eosin staining of differentiated UCX <sup>®</sup> spheroids resultant from <i>Reference Protocol</i>	37
Figure 15	Presence of HNF4 $\alpha$ , ALB and CK18 in the differentiated UCX <sup>®</sup> at day 24 and in undifferentiated UCX <sup>®</sup> in 3D culture method, detected by immunofluorescence staining.	37
Figure 16	Glycogen accumulation in differentiated UCX <sup>®</sup> resultant from <i>Reference Protocol</i> and Protocol C and undifferentiated UCX <sup>®</sup> in 3D culture method, determined by PAS staining	38
Figure 17	Urea production of differentiated UCX <sup>®</sup> resultant from <i>Reference Protocol</i> and Protocol C in 2D and 3D cell culture method at day 24.	39

## Glossary

3-MC	3-Methylcholanthrene
4-MU	4- Methylumbeliferone
AFP	$\alpha$ - fetoprotein
ALB	Albumin
ASC	Adult stem cells
BCA	Bicinchoninic acid
bmMSC	Bone marrow mesenchymal stem cells
BMP	Bone morphogenic protein
BSA	Bovine serum albumin
C/EBP $\alpha$	CCAAT-enhancer-binding proteins $\alpha$
C/EBP $\beta$	CCAAT-enhancer-binding proteins $\beta$
cDNA	Complementary deoxyribonucleic acid
CK18	Cytokeratin 18
CK19	Cytokeratin 19
CYP	Cytochrome
DAPI	4',6-diamidino-2-phenylindole
DMSO	Dimethyl sulfoxide
ECM	Extracellular matrix
ECOD	7-ethoxycoumarin- <i>O</i> -deethylase
EDTA	Ethylenediaminetetraacetic acid
EGF	Epidermal growth factor
ESC	Embryonic stem cells
FBS	Fetal bovine serum
FGF	Fibroblast growth factor
Foxa1-3	Forkhead box a1 to 3
GAPDH	Glyceraldehyde 3-phosphate dehydrogenase
GATA 4-6	GATA binding factor 4 to 6
Gp130	Glycoprotein 130
HGF	Hepatocyte growth Factor
HHEX	Hematopoietically-expressed homeobox protein
HLA	Human leukocyte antigen
HLC	Hepatocyte-like cells
HNF4 $\alpha$	Hepatocyte nuclear factor 4 $\alpha$
HNF1 $\alpha$	Hepatocyte nuclear factor 1 $\alpha$
H&E	Hematoxylin-Eosin
IFN- $\gamma$	Interferon $\gamma$
IMDM	Iscove modified dulbecco medium
iPSC	Induced pluripotent stem cells
ISCT	International Society for Cellular Therapy
ITS	Insulin–transferrin–sodium selenite
JAK/Stat3	Janus Kinase/Signal Transducer and Activator of Transcription 3
KLF4	Kruppel-like factor 4
MAPK	Mitogen-activated protein kinases
MSC	Mesenchymal stem cells
OCT 3	Octomer-binding transcription factor 3
OCT 4	Octomer-binding transcription factor 4
OSM	Oncostatin M



PCR	Polymerase chain reaction
P/S/A	Penicillin/streptomycin/ amphotericin B
PAS staining	Periodic acid Schiffs staining
PBS	Phosphate Buffered Saline
Pdx 1	Pancreatic and duodenal homeobox 1
PFA	Paraformaldehyde
Prox1	Prospero homeobox protein 1
qRT-PCR	Quantitative real-time polymerase chain reaction
ratPHep	Rat Primary Hepatocyte
RGD	Arginin-glycin-aspartic acid
RNA	Ribonucleic acid
RT	Room temperature
SD	Standard deviation
Sox17	Sry-related HMG box 17
STM	Septum transverse mesenchyme
TGF- $\beta$	Transforming growth factor $\beta$
Tm	Melting temperature
ucmMSC	Umbilical cord matrix mesenchymal stem cells
UGT	Uridine 5'-diphosphate glucuronosyltransferase
$\alpha$ -MEM	Minimum essential medium Eagle alfa modification

## 1. Introduction

### 1.1. Liver

The liver is the largest internal organ of the human body. It is populated by parenchymal and non-parenchymal cells. The hepatocytes, which are parenchymal cells, represent 60-70% of the total liver cells; whereas, the non-parenchymal cells include, hepatic endothelial cells, Kupfer cells, hepatic stellate cells and liver stem cells (oval cells) [1-2].

Concerning its organization, liver cells are encapsulated in a layer of connective tissue (Glisson capsule), being the organ divided in hepatic lobules which receive blood from the portal triad, the junction of three ducts that run in parallel: the intra hepatic biliary duct, portal vein and hepatic artery. The portal triad is surrounded by hepatocytes arranged in single cell sheets known as hepatic plates being the spaces between sheets of hepatocytes called sinusoid spaces, which are connected to a network of blood capillaries. Hepatic sinusoids lack a diaphragm and a basement membrane, which makes them much more permeable than other capillaries, even permitting the passage of plasma proteins with protein-bound nonpolar molecules, such as fat and cholesterol. This, combined with the plate structure of the liver, allow intimate contact between the hepatocytes and the contents of the blood [2, 15].

The products of digestion that are absorbed into blood capillaries in the intestine do not directly enter the general circulation, instead, this blood is delivered first to the liver, through the hepatic portal vein. The hepatocytes receive these digestive products in the form of glucose, amino acids, fatty acids and glycerol, and proceed to their metabolism. In glucose metabolism, part of the metabolic end products are stored in the liver and utilized when required. For instance, the liver in response to pancreas signalling plays an important role in the regulation of the blood glucose concentration by either removing glucose from the blood, by converting glucose into glycogen and triglycerides, or during fasting, by secreting glucose derived from the breakdown of stored glycogen in a process called glycogenolysis. It can also produce glucose by the conversion of noncarbohydrate molecules, such as amino acids, in a process called gluconeogenesis [1-2].

Another important liver function is the production of plasma proteins such as albumin and globulins. Albumin (ALB) is the main protein in the blood and is implied in regulation of oncotic pressure of the blood and in transport of hydrophobic molecules. On the other hand, globulins play a role in transport, inhibition of trypsin and blood clotting [2].

Hepatocytes are responsible for blood detoxification, by alteration of molecular structure through specific enzymes or by direct excretion in the bile. The urea cycle is the main process of blood detoxification, responsible for the conversion of ammonia, into urea, which is then excreted by the kidneys [2].

Hepatocytes can remove hormones and other biologically active molecules from the blood by excretion of these compounds into the bile. Bile is produced by hepatocytes and secreted into thin channels called bile *canaliculi*, located within each hepatic plate. These bile *canaliculi* drain into hepatic ducts that transport bile away from the liver. The liver can thus clear the blood of particular compounds by excreting them into the intestine in the form of bile, which are then eliminated in the faeces. The major constituents of bile are bile pigment (bilirubin), bile acids, phospholipids (mainly lecithin), cholesterol and inorganic ions [2].

## 1.2. *In vitro* toxicology models

Liver is the main organ for biotransformation. Hepatocytes possess phase I and II enzymes, responsible for the elimination and detoxification of xenobiotics. The cytochrome P450 enzymes are responsible for most phase I reactions, that are characterized by oxidative, reductive, and hydrolytic pathways where a functional group, *e.g.* hydroxyde, thiol and amine is added or exposed in the substrate. In phase II reactions, the newly introduced functional group is modified to O- and N-glucuronides, sulphate esters, various amides, and glutathionyl adducts, increasing polarity relative to the unconjugated molecules. This two-step transformation makes the substrates more water soluble, and therefore more easily excreted in urine [3].

Since liver is the main organ of biotransformation reactions, it is frequently affected by the drug side effects, which is the main cause of the withdrawal of an approved drug from the market. Thus, in order to avoid unexpected side effects of the novel drug, the availability of a good model for drug testing is essential [4].

*In vitro* models are commonly used for toxicology studies, these are: genetically modified bacteria or virus expressing various isoforms of cytochromes P450 [5-6], isolated perfused liver [1, 7], primary cultures of hepatocytes [1] and hepatic cell lines [9-10] .

The isolated perfused liver models are possible models to test hepatic metabolism, trans-hepatocellular transport and pharmacokinetics of drugs. These models have the advantage of maintaining structure and functional organization, mimicking the *in vivo* environment, however the complexity of the model difficult the understanding of intercellular processes, and also its functional integrity is lost after few hours [1, 7].

Thus, the most commonly used *in vitro* models are human hepatocellular carcinoma cell lines, such as HepG2 [10] and, more recently, HepRG [9]. HepG2 cell line is readily available, easy to handle and provide a reproducible human system [10]. However, this is not the ideal model since these cells are not in a completely mature state and thus drug metabolizing enzymes expression is different from normal functional hepatocytes.

HepRG is a human hepatoma cell line developed recently. These cells are able to differentiate from bipotent progenitor into mature hepatocyte-like cells (HLC) with the addition of 2% dimethyl sulfoxide (DMSO) and 50 $\mu$ M hydrocortisone hemisuccinate, resembling, more closely than HepG2, the adult hepatocyte cells. Mature HepRG express 85% of the genes expressed in primary human hepatocytes and levels of some CYP450 such as CYP3A4 and CYP2B6 and phase II enzymes are increased. Still, differentiated HepRG cells lack many important markers, for example C/EBP $\alpha$ , C/EBP $\beta$  and lack phase II enzyme UDP-glucuronosyltransferase (UGT) and important efflux pumps (bile salt export pump) [9].

Primary hepatocytes are a good model to enlighten the metabolic process of chemicals and effects of toxic agents in the liver. Freshly isolated hepatocytes preserve many

hepatic functions such as phase I and phase II enzyme activities, glucose metabolism and ammonia detoxification. Still, a continuous source of hepatocytes is needed to proceed to toxicology assays, which restricts the use of human primary hepatocytes for this type of studies, due to the shortage of available human liver material [1].

On the other hand, primary hepatocytes isolated from rat liver are more easily available and the results obtained are consistent, which make it good models for drug toxicology studies. Still, it has disadvantages: hepatic functions have interspecies differences, which cause differences in the hepatotoxicity reaction to drugs [4]. Besides, a problem which involve all primary cultures is the loss of specific-hepatic function after 48/72 hours, mainly of the biotransformation capacities [13] and plasma protein production [12]. Therefore, this loss of activity can be explained, among other things, by the culture method in which cells are cultured after isolation from the liver.

#### 1.2.1. 3D models

Traditionally, monolayer culture methods are applied to primary hepatocytes and cell lines, which implies the seeding of the cells in a flat surface forcing hepatocytes to acquire a flattened unnatural morphology [28]. However, *in vivo* cells possess three dimensional organization with complex cell-to-cell and cell-extracellular matrix (ECM) interactions, which hardly occur in a two dimensional culture support. This structure is of great importance to hepatocytes since they possess polar structure in the liver [2]. The 3D *in vivo* environment is mimicked through the use of 3D culture models, which utilization has grown in the past few years [29-30]. The 3D state can be achieved through several techniques, such as using scaffolds [30-31] and cell spheroids [11, 22, 28], among others [28].

3D scaffolds, which can be fabricated using synthetic or natural derivatives, allow the formation of a 3D environment without compromising gas, nutrient and metabolite exchange. These matrices can be adapted to different cell types by choosing the right rigidity and chemical structure. The chemical properties of the scaffold regulate the adhesion and spreading of cells. This is controlled by charge and polarity of the surface,

which dictate the diffusion and adsorption of proteins from the medium [32]. Cell adhesion can also be regulated, by integrating in the scaffold some structural components, *e.g.*, the incorporation of integrin ligand RGD permits the attachment of fibroblast cells [28].

On the other hand, the cell-spheroid technique is a simple 3D culture method that uses the capacity of some cells to self-assemble. It has the advantage of not requiring a scaffold and permitting an intricate cell-to-cell contact allowing the formation of ECM. The ECM is of great importance in maintaining hepatocyte functions during a longer time in culture. It allows the anchorage of hepatocytes and also induces intracellular signaling pathways [1]. However this method has some disadvantages: when spheroid thickness surpasses 1 mm, cells in the interior may lose contact with nutrients in the medium and accumulate toxic waste metabolites inside, forming a necrotic center [28].

3D cultures can be maintained in a static environment, where cells in spheroids or scaffolds are maintained in medium without agitation. The use of dynamic 3D cultures in bioreactor is also an alternative. Bioreactors allow the control of many environmental parameters such as: temperature, pH, medium flow rate, nutrient supply and toxic metabolite removal [28]. Many type of bioreactors are described and can be grouped in: rotating wall vessels, direct perfusion systems, hollow fibers, spinner flasks, and mechanical force systems [28]. Spinner flasks are a simple and effective method for culture of primary hepatocytes being able to maintain cellular functions, namely albumin secretion and biotransformation activity of phase I and phase II enzymes [11]. In this method cells can be seeded in scaffolds or allowed to form spheroids which dimensions can be controlled by the agitation rate. The agitation provided by the impeller result in higher homogeneity of the medium and quick dilution of toxic metabolites, while allowing a greater distribution of nutrients and oxygen and therefore reducing cell death [11].

### 1.3. Alternative models

A new possibility to replace primary cultures of hepatocytes in toxicology, consisting in hepatocyte-like cells (HLCs) derived from stem cells, recently appeared [4]. A stem cell is characterized by the capability to self-renew, dividing into two daughter cells, one of which retains its pluripotent abilities and allows the maintenance of the stem cells population; capacity of differentiating into tissues derived from all three germ layers, ectoderm, mesoderm and endoderm; and ability to renew a tissue in which it is inserted [26]. However, stem cells from different sources present different characteristics and not all meet the three criteria listed above. Stem cells which can only differentiate into multiple but limited lines of cells are termed multipotent stem cells or progenitor cells. Thus, due to its self-renewing capabilities and a strong proliferation rate many protocols have been developed in order to differentiate hepatocytes from stem cells. *In vitro* differentiation procedures aim at mimicking the development of hepatocytes *in vivo*, which consist in: (1) Endoderm induction; (2) Foregut and hepatic competence induction; (3) Hepatoblast and liver bud formation; (4) Differentiation of *hepatoblast* into hepatocyte.

#### 1. Endoderm Induction

*In vivo*, during gastrulation, the endoderm germ layer is established and emerges as a sheet of cells from the anterior end of the primitive streak [15]. Signalling by growth factor Nodal initiates endoderm and mesoderm formation in a concentration-dependent manner. Low doses of Nodal originate mesoderm formation and high doses originate endoderm formation. The transcription factors induced by Nodal are Sox17, and Foxa1-3, which regulate a cascade of genes responsible for the endoderm specification [33].

The endoderm induction step *in vitro* is based on the cell exposure to Activin A, a growth factor of the same family as Nodal, TGF- $\beta$  family [17, 33] (Table 1).

## 2. Foregut and hepatic competence induction

Endoderm then starts to form a primitive gut tube that is subdivided into foregut, midgut and hindgut. Each domain expresses a specific transcription factor: *hhex* in foregut, *pdx1* in the midgut and *cdx* in the hindgut. The embryonic liver originates from the ventral foregut endoderm. Gradients of fibroblast growth factor (FGF), Wnt, bone morphogenic protein (BMP) and retinoic acid secreted from the adjacent mesoderm are responsible for this patterning of endoderm [15, 34-36]. FGF and Wnt/ $\beta$ -catenin secreted from the posterior mesoderm repress foregut fate and promote hindgut development by inhibiting the expression of the *hhex* gene, essential for liver development. The absence of Wnt/ $\beta$ -catenin by its inhibition initiates liver development [35]. Only the foregut endoderm is competent to develop into the liver, possibly, due to the expression of transcription factors like *Foxa2*, *Gata4-6* and *Hhex* [37].

*In vitro*, this step is mimicked by exposing cells to growth factors such as FGF and epidermal growth factor (EGF), they activate the *hhex* gene expression [16, 25, 33-34] (Table 1).

## 3. Hepatoblast and liver bud formation

The foregut receives signals from the developing heart and septum transverse mesenchyme (STM), which releases FGF and BMP respectively. These signals induce hepatic fate in the ventral foregut endoderm [38-39].

After hepatic specification, cells start to express hepatic markers such as ALB,  $\alpha$ -fetoprotein (AFP) and HNF4 $\alpha$  and change their morphology from cuboidal to pseudostratified columnar epithelium, forming the liver bud. Then, the layer involving hepatic endoderm breaks down and the hepatoblasts migrate into STM. *Hhex*, *Gata 4*, *Gata 6*, *Prox1*, *Onecut-1* and *Onecut-2* are crucial in delamination process [15, 40]. At this stage the liver bud undergoes exponential growth and becomes the major site of fetal hematopoiesis. STM and hepatic mesenchyme secrete FGF, BMP, Wnt, retinoic acid and HGF, which promote hepatoblast proliferation and survival [15, 34, 39, 41].



Protocols in this step generally use FGF and BMP to mimic signals sent by the developing heart and STM, which induce a transformation in cell disposal and morphology [38-39]. Hepatocyte growth factor (HGF) is also commonly used in this step to promote hepatoblast proliferation and supplements like insulin–transferrin–sodium selenite (ITS) and nicotinamide, synergistically affect the hepatic driving pathway and can be used to help maintaining cells in culture [42] (Table 1).

#### 4. Differentiation of hepatoblast into hepatocyte

At this stage of differentiation, the hepatoblasts are bipotential and can differentiate into hepatocytes or biliary epithelial cells. Initially hepatoblasts express genes associated with adult hepatocytes such as *hnf 4 $\alpha$* , *albumin*, *ck18* and with biliary epithelial cells such as *ck19*, as well as with fetal liver genes such as AFP. Hepatoblasts in contact with the portal vein form a monolayer followed by a bilayer of cuboidal biliary precursors, increasing the expression of biliary genes and the down-regulation of hepatic genes [15]. Hepatoblasts that are not in contact with portal vein differentiate into mature hepatocytes. The factor responsible for the induction of hepatoblast differentiation into hepatocytes is oncostatin M (OSM) secreted by hematopoietic cells in the liver [43]. It induces metabolic maturation through gp130 and JAK/Stat3 signaling pathways [44]. These secreted factors regulate a number of liver-enriched transcription factors including C/EBP $\alpha$ , HNF1 $\alpha$ , Foxa1-3 and HNF4 $\alpha$ , which control hepatocyte gene expression [15, 45]. The maturation of hepatocytes and formation of extrahepatic bile ducts are gradual and this process continues until after birth [15].

*In vitro*, most protocols use factors such as OSM, and dexamethasone, which suppress growth and induce maturation of hepatocytes [43, 46] (Table 1).

**Table 1. Summary of *in vitro* differentiation protocols mimicking the *in vivo* liver development; gene expression checkpoints after each step of differentiation.**

DIFFERENTIATION STEPS	GROWTH FACTORS	GENE EXPRESSION CHECKPOINTS
Endoderm Formation	Activin A	Sox 17 Foxa1-3
Foregut and hepatic competence induction	EGF FGF	Hhex Gata 4-6 Foxa2
Hepatoblast and liver bud formation	FGF HGF BMP Nicotinamide ITS	ALB AFP HNF4 $\alpha$ CK18 CK19
Differentiation of hepatoblast into hepatocyte	OSM Dexamethasone	<b>Presence:</b> ALB CK18 HNF4 $\alpha$ C/EBP CYP3A4, 1B1, 1A1 <b>Absence:</b> AFP CK19

### **Embryonic stem cells (ESCs)**

Embryonic stem cells are derived from the inner cell mass of blastocysts and meet all the criteria for stem cells.

In the literature, protocols of differentiation of ESC into HLC are described. In summary, they consist in the differentiation into endoderm with Activin A and Wnt [47]. Then,

hepatoblast formation is induced by FGF and BMP, and maturation into hepatocytes is normally induced by HGF and OSM [16-19] (Table 1). Duan *et al.* (2007) proved the possibility of achieving differentiated ESC expressing liver-specific genes and exhibiting liver specific functions [19]. Moreover, Brólen *et al.* (2010) obtained HLC expressing the hepatic markers: CYP3A4, CYP1A2, CYP2C9,  $\alpha$ -1-antitrypsin, AFP, HNF4 $\alpha$ , CK18, ALB and exhibiting elevated urea secretion and glycogen accumulation. Finally differentiated cells had the ability to metabolize phenacetin, midazolam and diclofenac via the phase I cytochrome P450 enzymes, CYP1A, CYP3A and CYP2C, respectively [48]. However, increased tumorigenicity of these cells in *in vivo* models raise some problems in terms of safety [4, 49].

### **Adult stem cells (ASCs)**

Adult stem cells are multipotent stem cells present in many adult tissues, generating much less controversy among the scientific community. The liver contains a population of adult stem cells called oval cells. Liver progenitor cells are useful in the study of liver development and liver diseases, however, the stem cell isolation is difficult and provides low numbers of cells [4]. For oval cells to differentiate into HLCs, total confluence and addition of HGF and EGF or fibroblast growth factor-4 (FGF-4) is required, however a mature phenotype has not yet been achieved [50].

### **Induced Pluripotent Stem Cells (iPSCs)**

As it was proven for the first time by Takahashi *et al.* (2006,2007), it is possible to obtain pluripotent stem cells from human and mouse reprogrammed somatic cells [51-52]. This is achieved through the integration of the pluripotency genes OCT3/4, SOX2, KLF4 and c-MYC in the cell genome. Induced pluripotent stem cells (iPSCs) share many characteristics with ESCs and their use is ethically acceptable [51]. Differentiation procedures of iPSCs into HLCs are similar to protocols described to differentiate ESCs [23-24, 53]. Sullivan *et al.* showed the differentiation of iPSCs into cells exhibiting

hepatic markers ALB, AFP, HNF4 $\alpha$ , CYP71A, and with the capacity of secreting the plasma, and with CYP1A2 and CYP3A4 activity [23].

However, there are some problems concerning iPSCs, such as the variability caused by differences in the iPSCs reprogramming that can be the origin of the heterogeneity of the HLCs obtained [1].

### **Fetal stem cells**

Fetal stem cells are a more primitive population of stem cells that can be isolated from fetal tissues such as fetal blood as well as from umbilical cord blood and matrix. The use of fetal stem cells have advantages over ESCs and ASCs since their use is more ethically acceptable, have an enhanced multipotency and are less immunogenic than ASCs [54].

Mesenchymal stem cells (MSCs) are multipotent stem cells that can be isolated from fetal tissues such as umbilical cord blood and Wharton's jelly<sup>1</sup>. Many adult tissues also possess populations of MSC: adipose tissue, liver, muscle, bone marrow and dental pulp [55].

MSCs from different sources have been studied and each type varies in their proliferative and multilineage potential. However, the lack of a specific cell surface marker leads to difficulties in identifying this cell population.

Therefore, the Mesenchymal and Tissue Stem Cell Committee of the International Society for Cell Therapy (ISCT) proposes a set of standards to define human MSCs [56]:

1) MSC must be plastic-adherent when maintained in standard culture conditions using tissue culture flasks.

2) More than 95% of the MSC population must express CD105, CD73, CD90 and lack the expression of hematopoietic antigens CD45, CD34, CD14 or CD11b, CD79a or CD19 and HLA-DR molecules, not expressed on MSC unless stimulated (*e.g.* by IFN- $\gamma$ ).

3) Under specific stimuli, cells must be able to differentiate into osteoblasts, adipocytes, and chondroblasts *in vitro*.

These criteria apply only to human MSCs [56].

---

<sup>1</sup> Warton's Jelly is a gelatinous substance within the umbilical cord largely made up of mucopolysaccharides (hyaluronic acid and chondroitin sulfate). It contains a population of MSC.

MSCs, due to their immunosuppressive and anti-inflammatory characteristics, were considered a suitable model to cellular biology studies, tissue engineering and therapeutic application. Therefore, in the past few years their use has grown as well as the search of new sources, which can provide a higher cell number and less epigenetic damaged cells [55].

The differentiation process of MSCs is slightly different than ESCs or iPSC because MSCs are derived from mesoderm. However the reason these cells can be directed to hepatic fate is due to the expression of *hhex* gene in their genome. Thus, the endoderm induction step is not present in the majority of protocols described [20, 57-58].

UCX<sup>®</sup> cells are Wharton's Jelly derived human umbilical cord matrix Mesenchymal stem cells (ucmMSC). These cells meet the criteria for multipotent stem cells listed above [59]. UCX<sup>®</sup> isolation procedure allows for high numbers of cells, with less epigenetic damage [26-27]. Comparing with other adult sources of MSC, ucmMSCs have greater number of passages to senescence and shorter doubling times, which reflect the relatively primitive nature of these MSCs. [60].

UCX<sup>®</sup> have the ability to suppress T-cell proliferation in a more significant way than MSCs from other sources such as bmMSCs, and also have the capacity of convert naive CD4<sup>+</sup> CD25<sup>+</sup> T-cells into become regulatory by expressing the FOXP3 transcription factor, causing an immunosuppressive effect. Moreover, UCX<sup>®</sup> have anti-inflammatory effects in arthritis models *in vivo* [59].

Hence, UCX<sup>®</sup> are a great candidate to use as an alternative source in hepatic differentiation procedures to obtain models for *in vitro* toxicology. In spite of the advantages of ucmMSCs, to our knowledge, only one work, Campard et al. (2008), analysed the potential of these cells in the differentiation into HLC. The protocol described here was based in 3 steps that mimic the *in vivo* liver embryogenesis (see Annex 1). With this protocol, a population of differentiated cells with hepatocyte-like characteristics was obtained. Differentiated ucmMSC expressed hepatic markers: albumin, Glucose-6-phosphate, tryptophan 2,3-dioxygenase,  $\alpha$ -antitrypsin, tyrosine

aminotransferase and exhibited inducible CYP3A4 activity as well as glycogen accumulation, and urea production. However other important hepatic markers were present such as HepPar1, HNF4 $\alpha$  and CYP2B6, and  $\alpha$ -fetoprotein was present, which implies that a mature phenotype was not achieved.

#### 1.4. Objectives

In sight of the limitations with the current model systems for toxicological screening, this work intends to derive a ucmMSCs population (UCX<sup>®</sup>) into functional hepatocyte like-cells (HLCs).

In a first approach, a literature described protocol (Campard *et al.* (2008) [25]), for differentiating ucmMSCs into HLCs, will be tested in a UCX<sup>®</sup> population to assess their hepatocyte – differentiation potential.

In the search for a more efficient protocol, the above described procedure will be further optimized to generate a more effective and UCX<sup>®</sup>-directed procedure that results in hepatocyte-like cells. As we envisage to build a three-dimensional (3D) differentiated-cell system, the optimized protocol will be then implemented in this type of cultures to test their applicability in cell-differentiation.

Several functionality and biochemical endpoints will be used to characterize the obtained cell populations resultant from each protocol. These, as were never described for these type of cells, are first to be developed and include qRT-PCR techniques for specific genes and immunofluorescence assays for the detection of hepatocyte markers. Further more, other cell assays, including specific metabolic activity assays, must be tested and validated in the 3D cultures, to ensure their application in such models.

## 2. Materials and Methods

### 2.1. Cell culture reagents

Minimum essential medium Eagle alpha modification ( $\alpha$ -MEM), Iscove's modified dulbecco's medium (IMDM), epidermal growth factor (EGF), insulin-transferrin-selenium-premix (ITS), nicotinamide, dexamethasone, dimethyl sulfoxide (DMSO), penicillin/streptomycin/amphotericin B (P/S/A) and all other reagents, except when specified, were purchased from Sigma-Aldrich. Heat inactivated fetal bovine serum (FBS), 0.05% trypsin-EDTA solution, fibroblast growth factor-2 (FGF-2) and oncostatin M (OSM) were acquired from Invitrogen.

### 2.2. Collagen extraction and plate coating

The skin from frozen rat tails was removed using sterile scalpel and tweezers. Tendon fibers were pulled, separated from bone and cartilaginous tissue and suspended in PBS. Fibers were then washed three times and sterilized in 70% Ethanol for 1 hour before being transferred into 0.1% acetic acid and stirred during 48 hours at 4°C. The solution was centrifuged at 16000  $\times g$  for 90 minutes at 4°C. The supernatant was collected, lyophilized and the resultant solid stored at -80°C.

For collagen plate coating, lyophilized collagen was dissolved in a final concentration of 1 mg/mL in 0.1% acetic acid and diluted to 0.2 mg/mL in PBS. 0.5 mL of the solution was added to each well of 24-well plate, removed after 30 minutes and plates were left to dry.

For matrigel plate coating, Matrigel™ (BD Biosciences) was diluted 30x in  $\alpha$ -MEM and the solution was added to each well of 24-well plate, enough to cover the surface. Then matrigel™ (BD Biosciences) was removed and plates were left to dry.

### 2.3. Cell culture

The ucmMSCs (UCX<sup>®</sup>) were isolated by ECBio S.A., according to the procedure described in the patent (WO/2009/004379) “Optimized and defined method for isolation and preservation of precursor cells from human umbilical cord” developed by them.

For 2D cultures, UCX<sup>®</sup> were maintained in culture in T-flasks with  $\alpha$ -MEM supplemented with 10% FBS, herein designated as UCX<sup>®</sup> culture medium, and maintained at 37°C in a humidified atmosphere with 5% CO<sub>2</sub> in air. Seeding density was  $1 \times 10^4$  cells/cm<sup>2</sup>, and cells were trypsinized using 0.05% trypsin-EDTA solution every 3 days.

For 3D culture, UCX<sup>®</sup> were seeded in 6-well ultralow attachment plates (Nunc) in UCX<sup>®</sup> culture medium at a density of  $7.5 \times 10^4$  cells/cm<sup>2</sup>.

For the culture of Primary rat hepatocytes (ratPHep), these cells were seeded at a density of  $1.6 \times 10^5$  cells/cm<sup>2</sup>, after isolation, and maintained in culture with Williams E supplemented with 10% FBS, 1 mM sodium pyruvate (Lonza), 1% non-essential amino acid mixture (Lonza), 40  $\mu$ g/mL gentamicin, 100 U/mL penicillin/streptomycin/amphotericin B (P/S/A), 1.4  $\mu$ M hydrocortisone, 2 mM glutamine and 32 U/mL human insulin at 37°C in a humidified atmosphere with 5% CO<sub>2</sub> in air. Medium was replaced every day.

HepG2 cells were maintained in culture in T-flasks with  $\alpha$ -MEM supplemented with 10% FBS, 1 mM sodium pyruvate (Lonza), 1% non-essential amino acid mixture (Lonza), at 37°C in a humidified atmosphere with 5% CO<sub>2</sub> in air. Seeding density was  $2.5 \times 10^4$  cells/cm<sup>2</sup>, and cells were trypsinized using 0.05% trypsin-EDTA solution every 3 days.

Cell number was determined using a Neubauer counting chamber (Neubauer-modified, Brand) and cell viability was assessed with the trypan blue exclusion method.

### 2.4. BCA protein quantification

Protein concentration was determined using the BCA protein assay kit (Novagen) according to manufacturer instructions.

Briefly, cells in both 2D and 3D cell cultures were collected and disrupted by overnight incubation in 0.1 M NaOH solution at 37°C. 25  $\mu$ L of each sample in duplicate were mixed



with 200 µL BCA reagent and incubated at 50°C for 15 minutes, in a transparent 96-flat-bottom well plate. Absorbance at 592 nm was registered in a plate reader (Spectrostar Omega, BMG Labtech). Each sample concentration was determined with a standard curve of bovine serum albumin with concentrations ranging from 1000 to 25 µg protein per mL.

A linear calibration curve to relate total protein with cell number was also generated to estimate the UCX<sup>®</sup> cell number.

## 2.5. Hepatocyte differentiation protocols

For HLC differentiation, UCX<sup>®</sup> were seeded at a density of  $1.5 \times 10^5$  cells/cm<sup>2</sup> in 24-well plates (Nunc) coated as described in section 2.2. or inoculated at a density of  $7.5 \times 10^5$  cells/cm<sup>2</sup> in 6-well ultra low adherence plates (Nunc) (3D culture) in UCX<sup>®</sup> culture medium for 24 hours.

The HLC differentiation protocols (protocols A, B and C— see *Annex 1*) used in this thesis were developed based on the procedure described by Campard *et al.* (2008), that will be referred from this point beyond as *Reference Protocol* (see *Annex 1*). The *Reference Protocol* consists of 3 steps:

**Step 1:** 24 hours after inoculation, as described above, the UCX<sup>®</sup> culture medium was replaced for IMDM supplemented with 20 ng/mL of EGF, 10 ng/mL of FGF-2, 1% P/S/A and 2% FBS. This medium was maintained for two days.

**Step 2:** Culture medium was replaced by IMDM containing 20 ng/mL of HGF, 10 ng/mL of FGF-2, 0.61 g/L of nicotinamide and 1% ITS during 10 days.

**Step 3:** The third and last step of maturation consisted of treatment with IMDM containing 20 ng/mL of OSM, 1 µM of dexamethasone and 1% ITS for another 10 days. In the last two steps the medium was renewed every 2 to 3 days. The percentage of FBS and plate coating were optimized in this thesis work.

The Protocol A is a variant of *Reference Protocol*, with a modification in step 1 of differentiation. Step 1 of Protocol A consisted in induction of hepatic competence with

IMDM containing 20 ng/mL of EGF, 4 ng/mL of FGF-2, 1% P/S/A and 2% FBS for two days (*see Annex 1*).

Protocol B includes the modification of Protocol A with a further modification in step 2, which is the addition of 10 ng/mL of FGF-4 to differentiation media (*see Annex 1*).

Finally, Protocol C consists in Protocol B with the addition of 1% DMSO in the step 3 of differentiation (*see Annex 1*).

## 2.6. Quantitative real time polymerase chain reaction (qRT-PCR)

For RNA isolation, cells were detached using the standard trypsinization procedure and resuspended in Tryzol® (500 µL per  $0.5 \times 10^6$  cells; Invitrogen). Chloroform was added followed by centrifugation at 9000  $xg$  for 15 minutes at 4°C. The aqueous phase was collected and mixed with isopropanol. After centrifugation, cell pellet was washed with 75% ethanol in H<sub>2</sub>O-DEPC. After complete removal of ethanol, the pellet was dissolved in H<sub>2</sub>O-DEPC and the RNA concentration determined using spectrophotometry method at 260 nm (Spectrostar omega, BMG Labtech). The 260/280 nm and 230/280 nm, RNA/protein and solvent/RNA absorbance ratio, respectively, were used as purity control of the extracted RNA.

cDNA was synthesized from 1 µg RNA using Superscript® III Kit (Invitrogen) according to the manufacturer instructions. Briefly, the RNA mixed with 1 µL of oligo-DT (0.5 µg/µL) was kept at temperature of 70°C for 10 minutes. Then a mix with Superscript® III was added and the extension process was performed at 37°C for half an hour first and then the reaction was stopped at 65°C for 10 minutes. The synthesized cDNA was subjected to gene expression analysis using a quantitative reverse transcriptase-polymerase chain reaction (qRT-PCR). qRT-PCR was performed using the Power SYBR Green PCR Master Mix (Applied Biosystems) with the addition of power SYBR Green PCR Master Mix, forward and reverse primers, and 1 µg of template cDNA. Specific primers for hepatocyte genes were used: ck18 [61], ck19[61], alb [62], hhex [38] (*see Annex 2*). Optimal reaction conditions were 40 cycles of a two step PCR (denaturation at 95°C for 15 s; annealing at 60°C for 1 min and extension at 72° for 30 s) after an initial

denaturation step (95°C for 10 min). At the end of the reaction, a dissociation stage was added to determine the melting temperature ( $T_m$ ) of a single nucleic acid target sequence in an unknown sample in order to check if primer-dimer artifacts are forming and also to confirm the specificity of the reaction. The reaction was performed in the Real time PCR system (ABI7300; Applied Biosystems) fluorescence was measured at wavelengths 494 nm and 521 nm, excitation and emission, respectively. The Comparative CT Method ( $2^{\Delta\Delta CT}$ ) was used to quantify the amount of target genes, normalized to a reference gene *gapdh* [38]. The efficiency of each PCR reaction was estimated from a serially diluted HepG2 cDNA standard curve ( $10^0$ ,  $10^{-1}$ ,  $10^{-2}$ ) for the genes *ck18*, *alb*, *hhex* and a serially diluted UCX<sup>®</sup> cDNA standard curve for the gene *ck19*. UCX<sup>®</sup> and HepG2 were used as negative and positive controls, respectively.

## 2.7. Immunofluorescence

Cells cultured on collagen coated glass coverslips (13 mm diameter) were washed with 0.5 mM  $MgCl_2$  in PBS, and fixed with 4% paraformaldehyde (PFA) in PBS with 4% sucrose for 15 minutes and permeabilized afterwards with 0.3% Triton<sup>™</sup> X-100 in PBS for 15 minutes at RT.

Cell spheroids were collected from 3D cultures at the end of the differentiation procedures (day 24). Spheroids were resuspended in Tissue Tek<sup>®</sup> O.C.T. <sup>™</sup> (Sakura<sup>®</sup>) and cryosections of 10  $\mu m$  were prepared at the Histology Unit of *Instituto de Medicina Molecular* - UL. Cryosections were fixed in slides with acetone at -20°C and permeabilized with 0.08% Tween 20<sup>®</sup> for 15 minutes at RT.

The following steps were similar for both culture systems (2D and 3D). Nonspecific immunofluorescence was prevented by blocking with 0.2% fish skin gelatin/ 2% bovine serum albumin (BSA) in PBS for 30 minutes at RT. Fixed cells or cryosections were then incubated with primary antibody: mouse anti-human CK18 (Chemicon, CBL 177) and rabbit anti-human ALB (Santa Cruz Biotechnology, Inc.), diluted at 1:200 and 1:500, respectively, in 0.125% fish skin gelatin/ 1% BSA in PBS for 2 hours at RT shielded from the light.

The fixed cells or cryosections were then washed with PBS and incubated with secondary antibody: goat anti-mouse Alexa Fluor 488 and goat anti-rabbit Alexa Fluor 594 (Molecular Probes®) diluted in 1:500 in 0.125% fish skin gelatin in PBS with 0.1% Triton™ X-100, for 60 minutes at RT in the dark. ProLong® Gold anti-fade reagent with DAPI (4',6-diamidino-2-phenylindole; Molecular Probes) was used as mounting medium. Sample fluorescence was examined in fluorescence microscope at excitation, emission wavelengths of 590, 617 nm (Alexa Fluor 594), 495, 519 nm (Alexa Fluor 488) and 358,461 (DAPI). Images were recorded using Microscope Axio Scope.A1 coupled with a AxioCam HR and collected using AxioVision Rel. 4.7 software.

Rat primary hepatocytes one day after isolation and HepG2 served as positive controls while UCX® served as negative control.

## 2.8. Periodic acid Schiff's staining (PAS)

Cells and cryosections (spheroids were sectioned as described in section 2.7) were fixed with 4% PFA in PBS or with acetone, respectively, and incubated with 1% periodic acid in PBS for 10 minutes, washed with distilled water, and incubated with Schiff's reagent for another 15 minutes. After washing with distilled water, Mayers' hematoxylin counterstain was performed for 30 seconds and the preparations washed and visualized in an inverted microscope (Olympus CK30). Data images were recorded using Moticam 2500 and collected using Motic Images Plus V2.0 software.

Freshly cultured ratPHep and HepG2 served as positive controls while UCX® served as negative control. Inner control consisted of differentiated HLCs treated with 1 g/L of amylase in CaCl<sub>2</sub> 30mM, for 15 minutes at 37°C after fixation.

## 2.9. Hematoxylin-Eosin staining (H&E)

For hematoxylin and eosin (H&E) staining, cryosections were first stained with Harris's hematoxylin for 10 min and rinsed with deionized water. After an incubation step with HCl 1% (v/v) in 70% EtOH, slides were stained with Eosin Y for 2 min. Slides were then submitted to increased concentrations of ethanol and finally incubated in xylene (EMD

Chemicals). Samples were mounted with Entellan® (Merck). Images were acquired as described in 2.8.

## 2.10. Urea production

The urea production rate was determined by quantification of urea in culture supernatant using a quantitative colorimetric urea kit (QuantiChrom™ Urea Assay Kit, DIUR-500, BioAssay Systems), according to the manufacturer's instructions. Sample absorbance was measured at 520 nm in a microplate reader (Spectrostar omega, BMG Labtech). A standard sample absorbance was simultaneously measured and the concentration of samples was determined according to formula described in manufacturer's instructions. The results were normalized to control (culture medium) expressed as  $\text{mmol}/10^6 \text{ cells.h}$ . UCX® were used as negative controls, while HepG2 and ratPHep (one day after isolation) were used as positive controls.

## 2.11. 7-ethoxycoumarin-*O*-deethylase (ECOD) activity

The following procedure was adapted from Castell and Gómez-Lechón, 1997 and focuses on human CYP2B6, 1A2 and 2E1 activity [30].

After 3 day induction with 3-methylcholanthrene (3-MC), cells were exposed to culture media containing 7-ethoxycoumarin (0.8 mM) and salicylamide (1.5 mM) for 90 minutes at 37°C. After incubation time, samples were immediately collected and chilled on ice. Cells and debris were removed by centrifugation at 9000  $\times g$  for 2 minutes at 4°C, and the supernatant samples stored at -80°C. Cell monolayer was treated as described in issue 2.4.

For the determination of 7-hydroxycoumarin, the stored supernatant was extracted with equal volume of chloroform. The organic phase was back-extracted with an equal volume of 5.84% of NaCl in 0.1M NaOH solution. 200  $\mu\text{l}$  of aqueous alkaline phase were transferred in duplicate to opaque 96 well-plate. The samples fluorescence was measured in a plate reader (Fluorostar Omega, BMG Labtech) with excitation and emission wavelengths of 340 nm and 460 nm respectively and recorded with Omega 3.0

and MARS data analysis 2.41. The obtained values were calculated using a calibration curve of 7-hydroxycoumarin ranging from 0 to 12  $\mu\text{M}$ , and normalized to the control (medium with substrate). ECOD activity was expressed as  $\mu\text{M}$  of 7-hydroxycoumarin formed per hour per  $10^6$  cells. ECOD activity in UCX<sup>®</sup> was considered negative control while activity in HepG and in ratPHep (one day after isolation) served as positive controls.

### 2.12. Uridine 5'-diphosphate glucuronosyltransferase (UGT) activity

Uridine 5'-diphosphate glucuronosyltransferase (UGT) activity was determined by quantification of the substrate, 4-methylumbelliferone (4-MU), before and after cell incubation. The procedure was performed according to Gomez-Léchon et al. (1997) with slight modifications [30]. Briefly, 100  $\mu\text{M}$  solution of 4-MU in PBS were incubated with differentiated UCX<sup>®</sup> for 1h at 37°C, 5% CO<sub>2</sub> in air humidified atmosphere. The supernatant was collected and chilled on ice. Cell and debris were removed by centrifugation at 9000  $\times g$  for 2 minutes at 4°C. Cell monolayer was treated as described in issue 2.4.

After centrifugation, samples were transferred into a black 96-well plate and fluorescence was analysed at an excitation wavelength of 360 nm and emission of 460 nm in plate reader (Fluorostar omega, BMG Labtech) and recorded using Omega 3.0 and MARS data analysis 2.41. The 4-MU remaining concentration was determined based on a standard curve of 4-MU with concentration ranging from 100 to 0  $\mu\text{M}$ . The activity was expressed as  $\mu\text{M}$  of 4-MU metabolized per hour per  $10^6$  cells. UGT activity in UCX<sup>®</sup> was used as negative control while HepG2 and ratPHep one day after isolation were used as positive controls.

### 2.13. Statistical analysis

The results are given as the mean  $\pm$  SD. Statistical data analysis were performed using PRISM 2.01 (GraphPad Software). Data were compared by means of Student's two-sided t-test, and a P-value lower than 0.05 was considered significant.

### 3. Results

Many protocols have been used to differentiate MSC from different sources into hepatocyte-like-cells (HLCs). However, little investigation has been made in the differentiation of ucmMSCs cells and the results obtained were unsatisfactory. In this work (i) optimization/development of a protocol for differentiating UCX® into hepatocytes was primarily performed in 2D culture conditions and a (ii) further approach was to adopt the optimized protocol to 3D spheroid cultures in order to achieve a more homogenous and functional population of HLC.

To our knowledge only one study has reported successful human ucmMSCs differentiation into HLC. This work is the one described by Campard et al. (2008). However, absence of some hepatic markers in differentiated UCMSCs, as HepPar1 or hepatocyte nuclear factor 4 (HNF4 $\alpha$ ), implied that their differentiation did not reach the level of mature hepatocytes. In any case, the differentiation protocol used in this study will be our starting point, and will be herein referred as *Reference Protocol*. Other protocols, derived from the *Reference Protocol*, were also implemented and evaluated. Thus, UCX® were submitted to several *in vitro* differentiation protocols based on successive exposure to hormones, growth factors, cytokines and chemicals, mimicking the liver development. The differentiated UCX® were characterized regarding cells morphology, the expression of specific hepatic markers and its metabolic activity. Undifferentiated UCX® were used as negative control and HepG2 and rat primary hepatocytes (ratPHep) as positive controls.

The expression patterns of the hepatic markers ALB, CK18 and HNF4 $\alpha$  were determined through qRT-PCR and immunofluorescence. The expression of *ck19*, which must be absent in differentiated UCX®, was also analysed by qRT-PCR.

Moreover, the glycogen accumulation capacity, biotransformation activity and detoxification of ammonia, metabolic functions performed by hepatocytes, were evaluated. The glycogen accumulation capacity was detected with periodic Acid Schiff's staining; the biotransformation activity was measured by ECOD assay (phase I enzymes)

and UGT assay (phase II enzymes); finally, ammonia detoxification capacity was assessed by the quantification of urea present in cells supernatant.

### 3.1. UCX<sup>®</sup> differentiation into hepatocyte- like cells under 2D conditions

#### 3.1.1. Optimization of coating, seeding density and FBS concentration

The optimal conditions for UCX<sup>®</sup> differentiation into hepatocyte-like cells were first determined. We tested the effect of different coatings (Matrigel™ [61], rat tail collagen [25, 61] and no coating) described for hepatocyte culturing [25, 61] and the percentage of FBS used in the hepatocyte differentiation (0%, 2%, 5% and 2%/0%). During the differentiation protocol cells should remain adherent and viable, being the plate coating and the percentage of FBS adopted, of great importance. Because differentiation requires cell cycle arrest, we also tested the effect of cell density ( $1 \times 10^4$  cells/cm<sup>2</sup>,  $1.5 \times 10^4$  cells/cm<sup>2</sup> and  $2 \times 10^4$  cells/cm<sup>2</sup>). Cells must be at 70-80% confluence at the beginning of the differentiation and thus, the correct seeding density has to be evaluated. To demonstrate differentiation to HLC, the protocol described by Campard *et al.* (2008), *Reference Protocol*, was applied and cell morphology at day 24 of differentiation was assessed.

Since most differentiation protocols are performed in serum free culture medium the coating evaluation was performed in UCX<sup>®</sup> inoculated in serum free media [20-21]. In plates with Matrigel™ coating it could be observed that UCX<sup>®</sup> detached from the plate surface after 2 weeks in culture, not enabling the completion of the UCX<sup>®</sup> differentiation (Fig. 1); whereas, rat tail collagen coating allowed a better attachment of cells at inoculation and the maintenance of adherent cells during the whole differentiation period that lasted 24 days (Fig. 1).

The FBS percentages tested were 0%, 2% and 5% during all differentiation process and 2% in the first step (2 days) with a reduction to 0% FBS throughout the rest of the differentiation protocol. The last condition was the most successful because it enabled



cell adaptation to a media without FBS, and cells show a more pronounced epithelial morphology at the end of the differentiation (Fig. 1).

Finally, when cell densities between 1 and  $2 \times 10^4$  cells/cm<sup>2</sup> were tested, a confluence of 70% at the beginning of differentiation, i.e., 1 day after cell inoculation was obtained with a cell seeding density of  $1.5 \times 10^4$  cells/cm<sup>2</sup>.

Therefore, the collagen coating and seeding density of  $1.5 \times 10^4$  cells/cm<sup>2</sup> in medium supplemented with 2% FBS, followed by medium replacement for FBS free medium after 2 days were the optimal conditions for UCX<sup>®</sup> differentiation and were further applied in the following work.

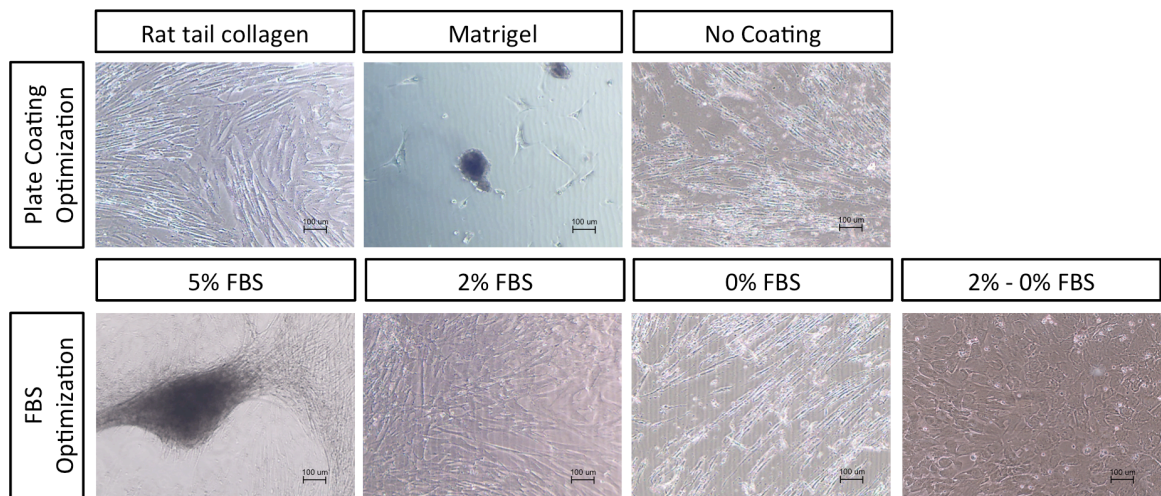


**Figure 1.** Morphology of differentiated UCX<sup>®</sup> resultant from *Reference Protocol* with different plate coatings (rat tail collagen, Matrigel<sup>®</sup>, without coating) and FBS concentrations (5% , 2%, 0% and 2% in step 1 and 0% in steps 2 and 3). All images were acquired at day 24 of differentiation for the exception of Matrigel<sup>®</sup> and 5% FBS optimization that were acquired at day 16 and 22, respectively.

### 3.1.2. Induction of hepatic competence

Considering the *Reference Protocol* as a starting point, several modifications to this protocol were performed step by step in order to improve the hepatogenic phenotype of the HLCs derived from UCX<sup>®</sup>.

Two FGF-2 concentrations were tested in the step of differentiation: 4 ng/mL (Protocol A, see annex 1) and 10 ng/mL (*Reference Protocol*). *hhex* expression, checkpoint of the first step, was evaluated through qRT-PCR. As shown in figure 2, UCX® in the presence of 4 ng/mL of FGF-2 in the first differentiation step (Protocol A), resulted in a 20-fold increased expression of *hhex* when compared to the *Reference Protocol* (Fig. 2), which indicates that a lower concentration of FGF-2 is inducer of *hhex* expression.

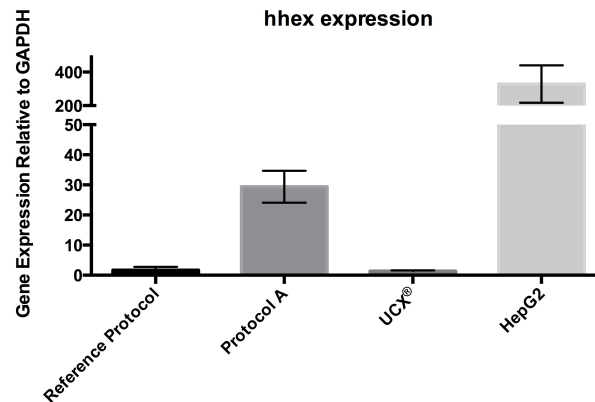


**Figure 2.** Relative *hhex* gene expression of differentiated UCX® resultant from *Reference Protocol* and Protocol A at day 2, of undifferentiated UCX®(negative control) and HepG2 (positive control), determined by qRT-PCR. *hhex* gene expression was normalized to GAPDH.

### 3.1.3 Characterization of the Differentiation Pattern of UCX® into epatocyte-like Cells (HLCs): *Reference Protocol*, *Protocol A*, *Protocol B* and *Protocol C*

Previously, it has been shown that ucmMSCs could differentiate into HLCs upon sequential exposure to a mixture of well-defined cytokines and growth factors (*Reference Protocol*, Campard et al. 2008)[25]. However, a non-mature population of HLC was obtained. In an attempt to improve the differentiation of UCX® into HLC, cells were exposed to the same well-defined hepatogenic factors, but with alterations in each of the three differentiation steps. More specifically, Protocol A consisted in the alteration of the FGF-2 concentration from 10 ng/mL to 4 ng/mL in step 1 of

differentiation, Protocol B in the addition of FGF-4 (10 ng/mL) to the step 2 of differentiation and Protocol C to the addition of DMSO (1%) to the step 3 of differentiation.

### **Cells morphology**

As observed in figure 3, cellular morphology changes were evident in all protocols.

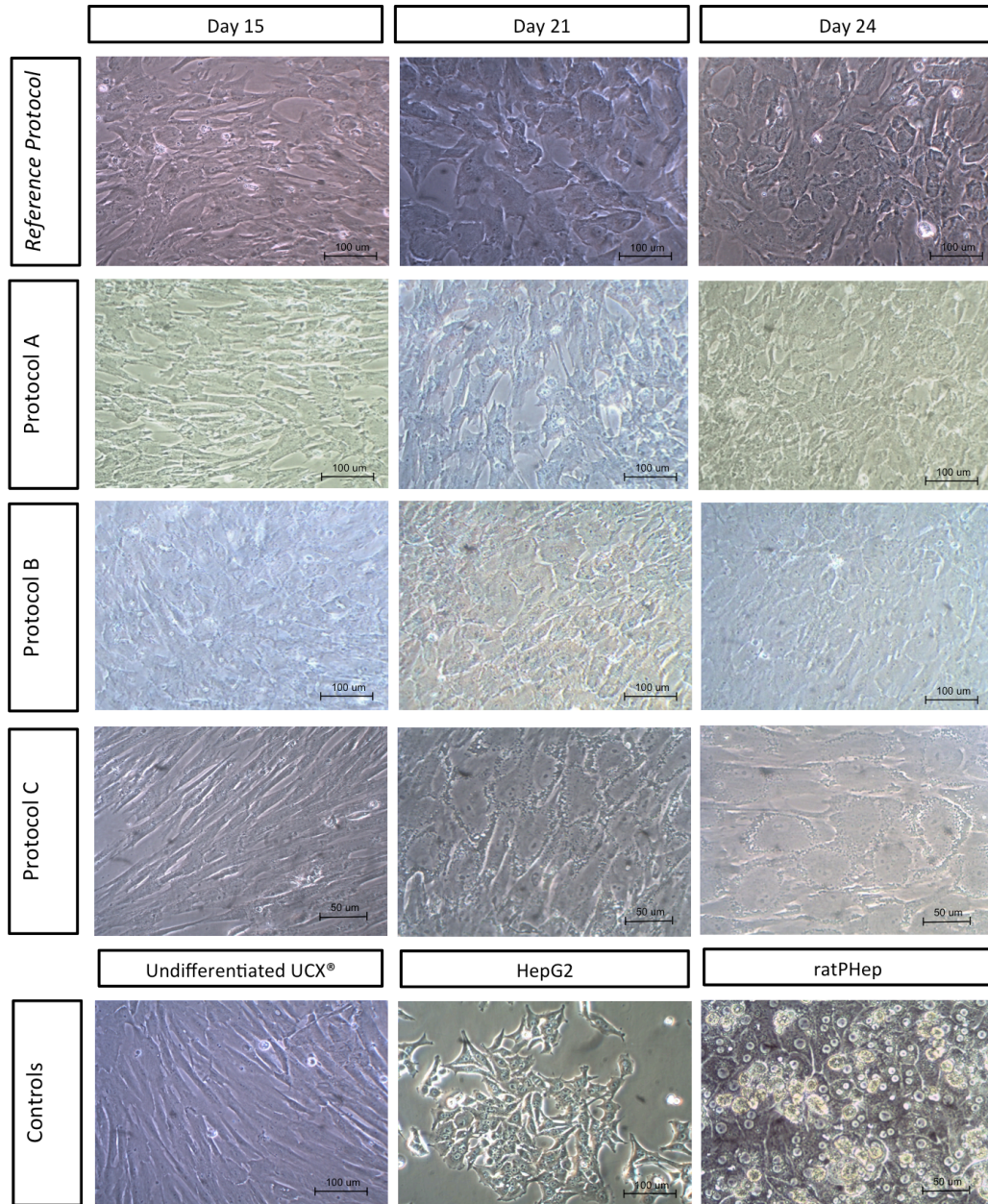


**Figure 3. Morphology of differentiated UCX® at days 15, 21 and 24 and of undifferentiated UCX®, HepG2, and ratPHep (one day after isolation) in 2D culture method. Magnification: 20x.**

While, undifferentiated UCX<sup>®</sup> showed an elongated fibroblastoid morphology, with wide cytoplasm, differentiated UCX<sup>®</sup> (from *Reference Protocol*, Protocols A, B and C) showed a polygonal epithelial morphology with a granular cytoplasm and many cells were binucleated. To be noted that the polygonal shape could be observed in all protocols from day 17 onwards (Fig. 3).

### **Characterization at the molecular level**

The hepatocyte differentiation was further evaluated by immunofluorescence and qRT-PCR for early (CK19) and late (CK18, albumin, HNF4 $\alpha$ ) markers of hepatocyte differentiation.

The ck19 biliar marker expression, which must be absent in fully differentiated hepatocytes, was assessed in undifferentiated UCX<sup>®</sup> and differentiated UCX<sup>®</sup> collected at day 24 of differentiation. A clear down regulation of *ck19* expression of differentiated UCX<sup>®</sup>, from all protocols, when compared to undifferentiated UCX<sup>®</sup> was observed (Fig. 4).

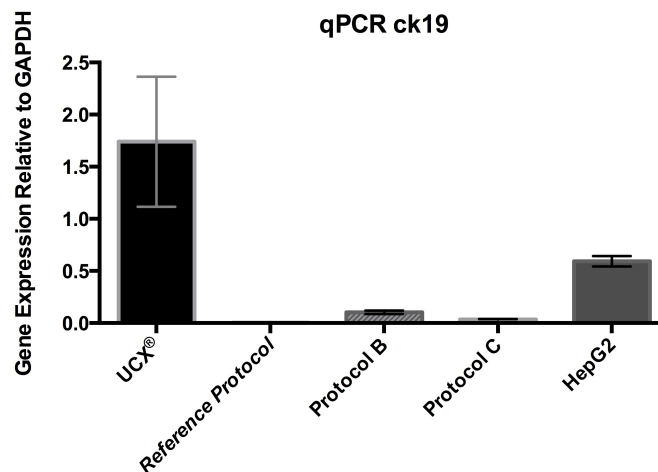


**Figure 4.** Relative *ck19* gene expression of differentiated UCX<sup>®</sup> resultant from *Reference Protocol*, Protocol B and C at day 24 and of undifferentiated UCX<sup>®</sup> and HepG2 determined by qRT-PCR. *ck19* gene expression was normalized to GAPDH



In contrast, later markers such as *alb* and *ck18* were highly expressed in both differentiated UCX<sup>®</sup> and HepG2, though more pronounced in the differentiated cells (Fig. 5). Both the pattern and the level of expression, however, differed between the culture methods. In fact, upon exposure to Protocol C, maximal *alb* expression was observed, with an approximately 20 times fold increase when compared to both HepG2 cells or differentiated UCX<sup>®</sup> using the *Reference Protocol*. *ck18* expression, on the other hand, reached maximal levels in both differentiated UCX<sup>®</sup> exposed to Protocols B and C, about 2-fold and 7-fold higher than the levels observed in the undifferentiated UCX<sup>®</sup> and HepG2, respectively (Fig. 5). Undifferentiated UCX<sup>®</sup> exhibited a low expression of the hepatic markers *ck18* and *alb*.

Thus, UCX<sup>®</sup> exposed to the differentiation protocols underwent a consecutive array of developmental stages comparable with *in vivo* hepatogenesis.

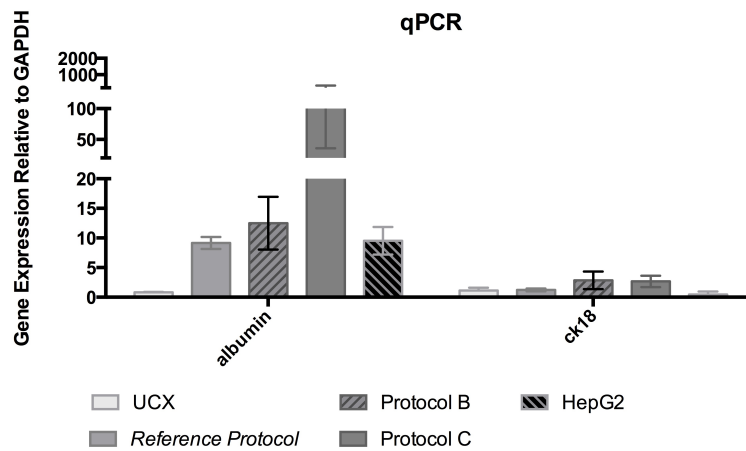


**Figure 5. Relative *alb* and *ck18* gene expression of differentiated UCX<sup>®</sup> resultant from *Reference Protocol*, Protocol B and C at day 24 and of undifferentiated UCX<sup>®</sup> (negative control) and HepG2 (positive control) determined by qRT-PCR. *alb* and *ck18* gene expression were normalized to GAPDH.**

The qRT-PCR results were further supported by immunofluorescence analyses. Immunofluorescence showed the presence of the characteristic hepatic markers, ALB, CK18 and HNF4 $\alpha$  in all differentiated UCX<sup>®</sup>, as well as in the positive controls (HepG2 and ratPHep). These markers were not detected in the undifferentiated UCX<sup>®</sup> (Fig. 6-7). Moreover, HNF4 $\alpha$  is not present in ucmMSCs differentiated into HLSCs using the *Reference Protocol* [25].

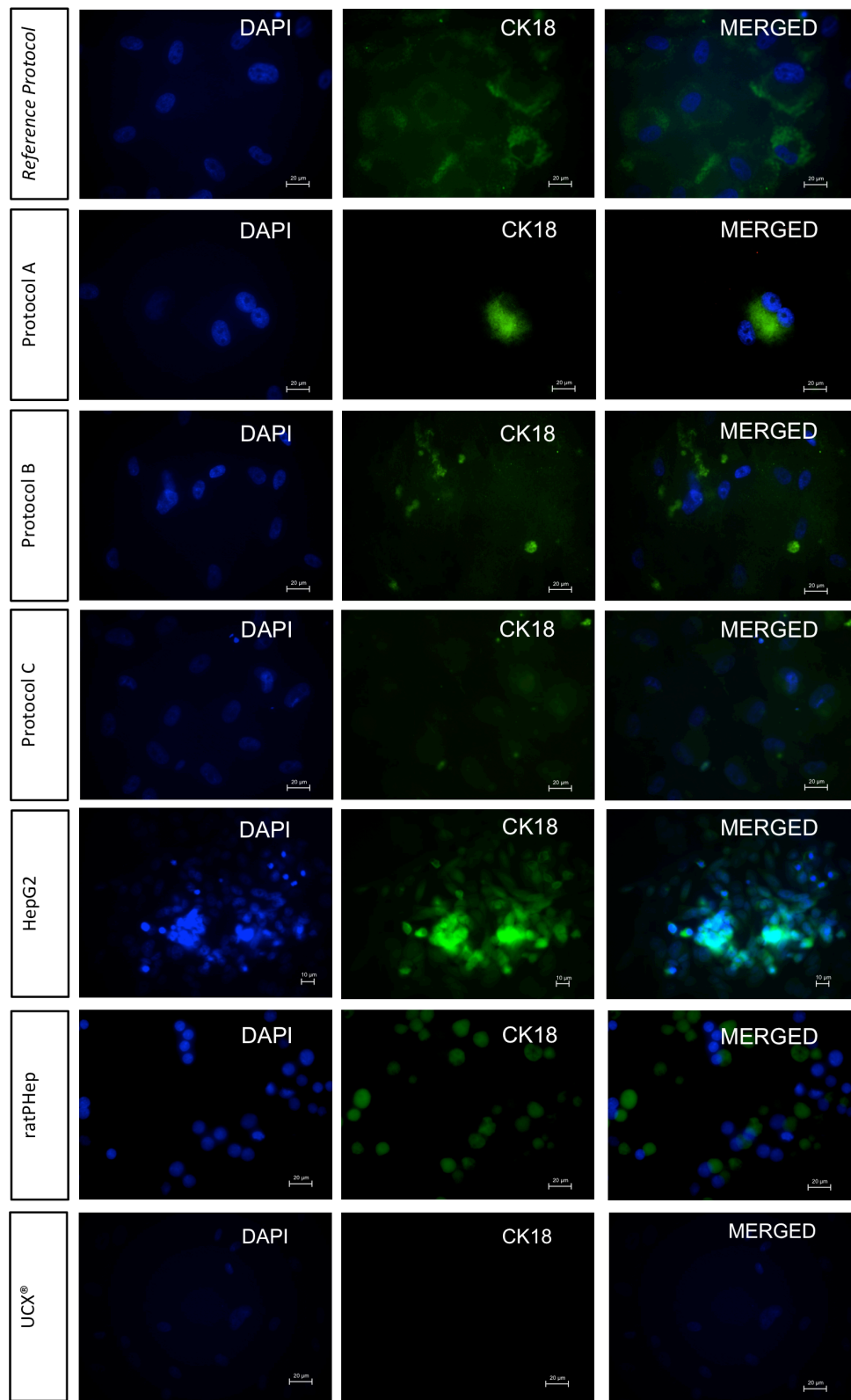


**Figure 6.** Presence of CK18 in differentiated UCX® at day 24, in undifferentiated UCX®(negative control), ratPHep (one day after isolation) and HepG2 (positive controls) in 2D culture method, detected by immunofluorescence staining. Magnification: 63x, except for HepG2 images (40x).

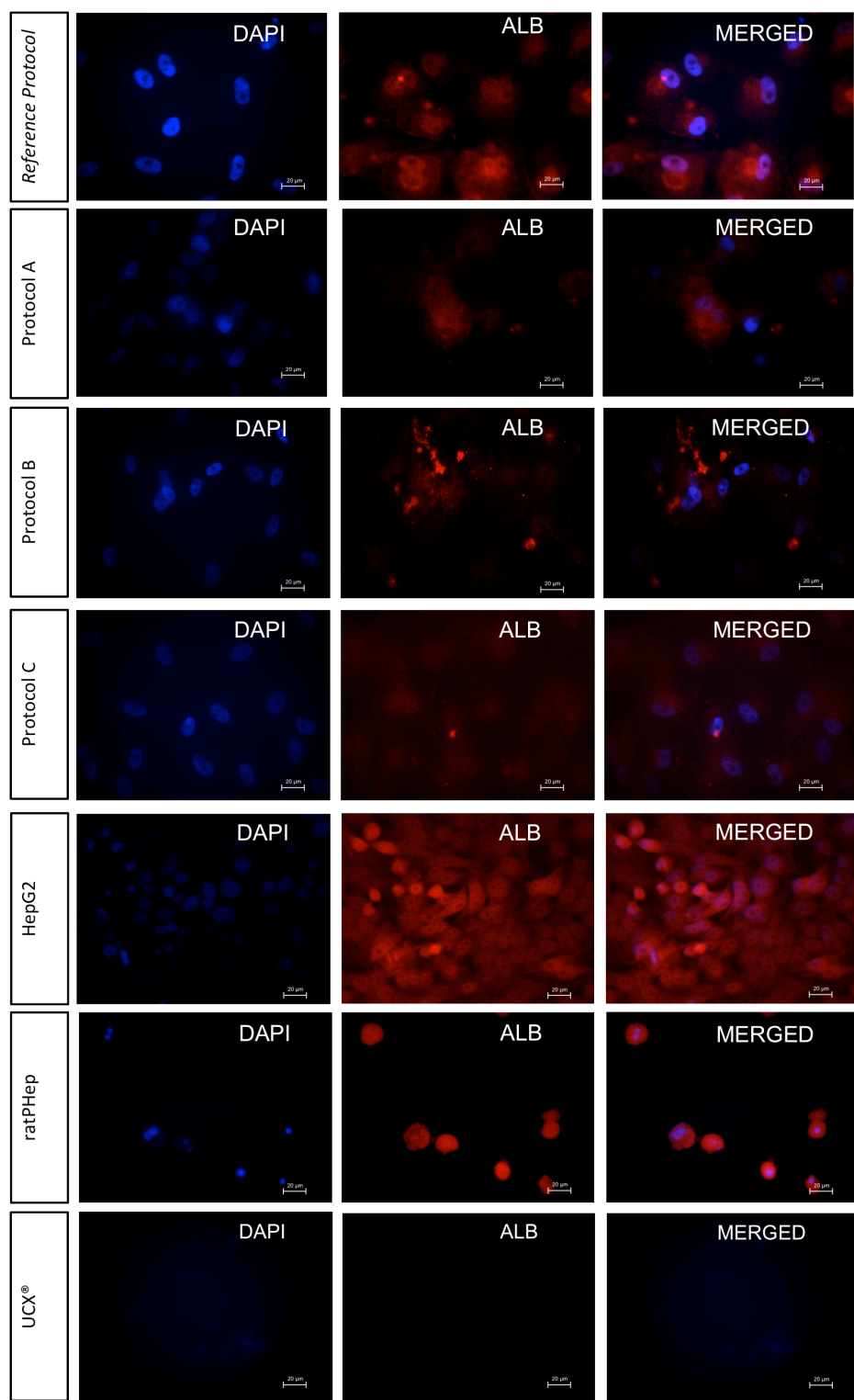


Figure 7. Presence of ALB in differentiated UCX® at day 24, in undifferentiated UCX®(negative control), ratPHep (one day after isolation) and HepG2 (positive controls) in 2D culture method, detected by immunofluorescence staining. Magnification: 63x

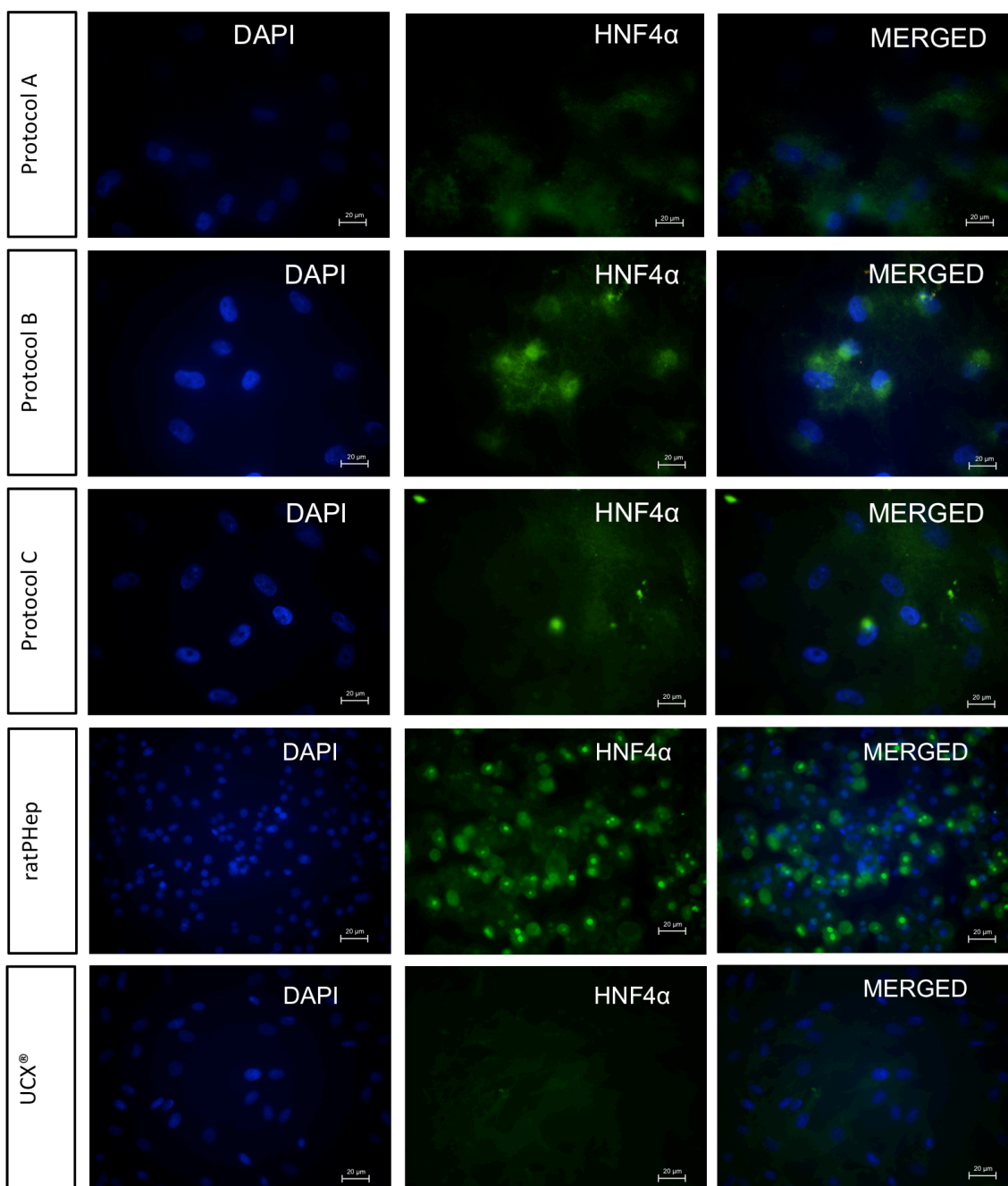


Figure 8. Presence of HNF4 $\alpha$  in the differentiated UCX® at day 24, in undifferentiated UCX® (negative control), ratPHep (one day after isolation) and HepG2 (positive controls) in 2D culture method, detected by immunofluorescence staining. Magnification: 63x.

### ***Phase I and II enzymes activity***

Phase I and II enzymes activity of the differentiated UCX® was evaluated by means of ECOD activity and UGT, respectively. ECOD activity was evaluated at day 24 of



differentiation in the presence and absence of the 3-MC inducer (Fig. 9). As expected, no ECOD activity could be observed in undifferentiated UCX<sup>®</sup>. Similarly, no activity could be detected in UCX<sup>®</sup> exposed to the *Reference Protocol*. In contrast, in the absence of 3-MC, all differentiated UCX<sup>®</sup> exhibited ECOD activity similar (with no significant differences) to ratPHep.

CYP-inducibility is considered as the most representative metabolic function of the adult hepatic phenotype [63]. Therefore, the responsiveness of CYP1A1/2, CYP2A1/2 and CYP2B1/2 to their respective inducer 3-MC was analyzed in parallel. ECOD activities were inducible when using protocols B (1.5-fold), C (10.8-fold) and in ratPHep (12-fold) after 3-day exposure to 3-MC (i.e., on day 21) (Fig. 9).

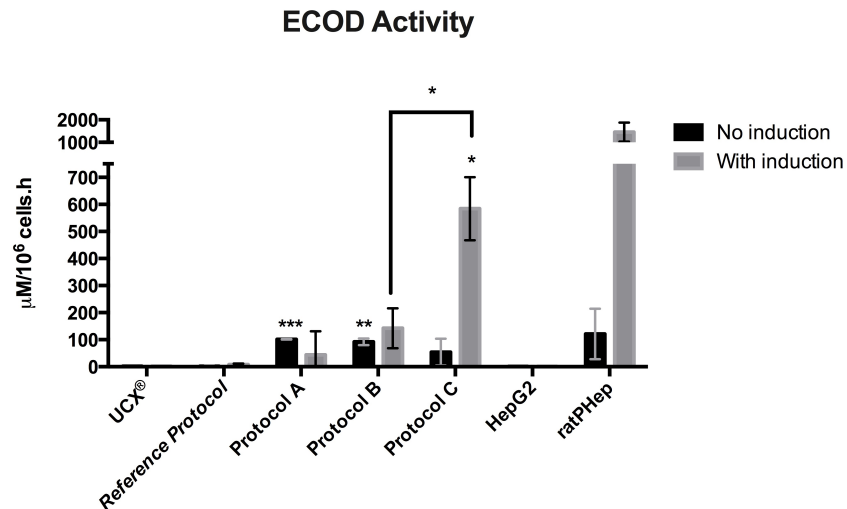


Figure 9. ECOD activity of differentiated UCX<sup>®</sup> at day 24 and of undifferentiated UCX<sup>®</sup> (negative control), HepG2 and ratPHep (one and four days after isolation) (positive controls) in 2D culture method. Data is represented as the mean  $\pm$  SD. \* $p$ <0.05, \*\* $p$ <0.01, \*\*\* $p$ <0.001. The ECOD activity of differentiated UCX<sup>®</sup> from protocols A, B and C was compared with *Reference Protocol* ( $n=2$ ).

UGT activity of all differentiated UCX<sup>®</sup> was significantly higher than ratPHep and HepG2 cell line (Fig. 10). Protocols B and C at day 24, exhibited significantly higher UGT activity than *Reference Protocol* (Fig. 10). Moreover, undifferentiated UCX<sup>®</sup> showed some level of UGT activity, but, much lower than differentiated cells.

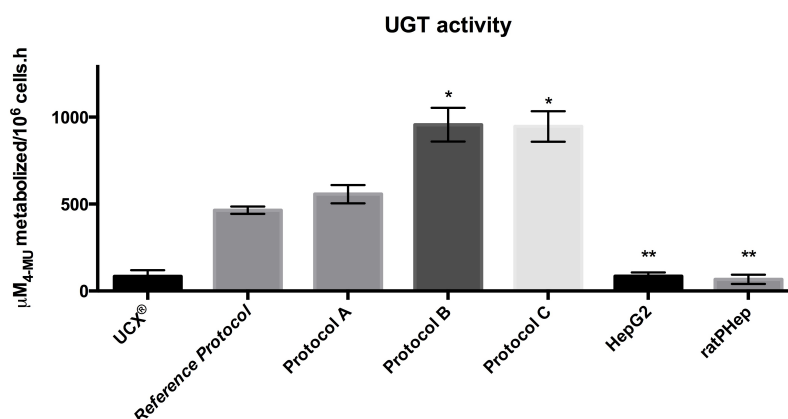


Figure 10. UGT activity of differentiated UCX® at day 24 and of undifferentiated UCX® (negative control) and HepG2, ratPHep (one day after isolation) (positive control) in 2D culture method. Data is represented as the mean  $\pm$  SD. \* $p < 0.05$ , \*\* $p < 0.01$ . The UGT activity from protocols A, B, C was compared with *Reference Protocol* ( $n=2$ ).

### Urea production

Differentiated cells from *Reference Protocol* exhibited lower urea production relative to positive controls. However, when compared to HepG2 increased urea production could be obtained with UCX® exposed to Protocols A, B or C. The same urea production levels were measured in ratPHep (Fig. 11).

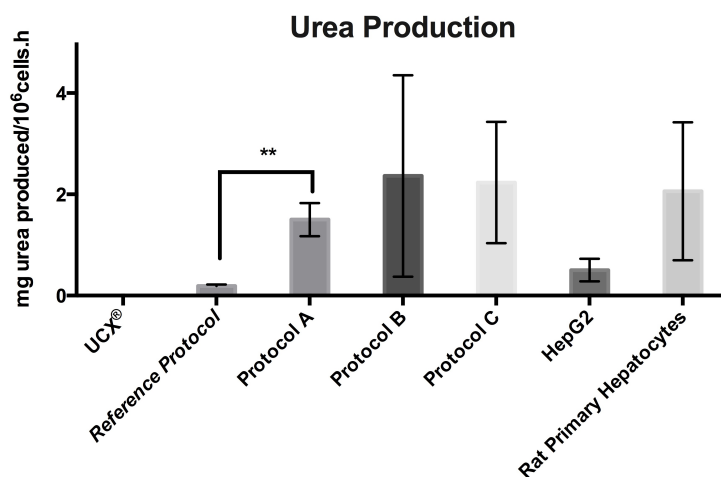
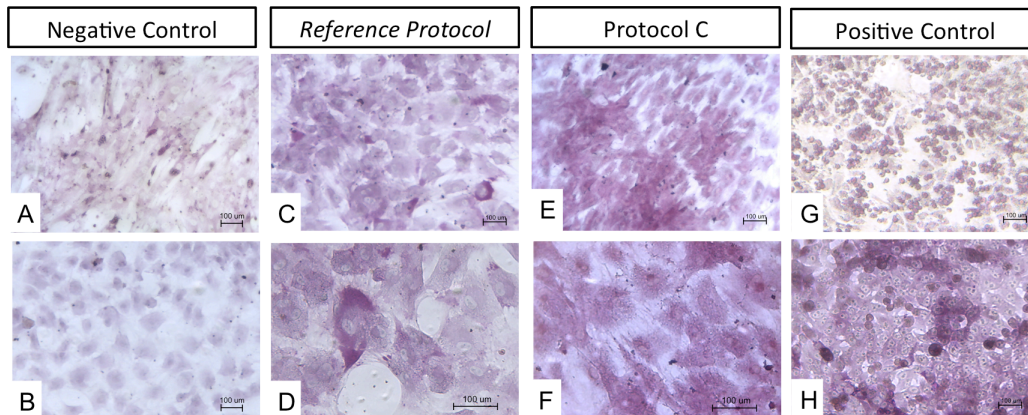


Figure 11. Urea production of differentiated UCX® at day 24 and of undifferentiated UCX® cells (negative control), in HepG2 and ratPHep (one day after isolation) (positive control) in 2D culture method. Data is represented as the mean  $\pm$  SD. \* $p < 0.05$ , \*\* $p < 0.01$  ( $n=2$ ).

Moreover, differentiated UCX® from day 24 exposed to Protocol A and Protocol C showed a superior urea secretion than *Reference Protocol*, although the results could only be significant regarding Protocol A (Fig. 11).

### **Glycogen Storage**

Glycogen accumulation capacity was assessed through PAS staining in differentiated UCX® from *Reference Protocol* and in differentiated UCX® from Protocol C, the protocol with best results. All differentiated UCX® (Fig. 12C-F) showed accumulation of glycogen in its cytoplasm such as ratPHep (Fig. 12G) and HepG2 (Fig. 12H), while undifferentiated UCX® did not revealed glycogen storage (Fig. 12A). Indeed, staining was specific for glycogen because treatment of differentiated UCX®, exposed to *Reference Protocol*, with amylase prevented a positive reaction (Fig. 12B).



**Figure 12.** Glycogen accumulation in differentiated UCX® at day 24 and in undifferentiated UCX®, HepG2 and ratPHep (one day after isolation) in 2D culture method revealed by PAS staining. (A) Undifferentiated UCX®; (B) Amylase treatment in differentiated UCX® exposed to *Reference Protocol*; (C, D, E, F) Differentiated UCX®; (G) ratPHep; (H) HepG2. Magnification: 10x, except for D and F (20x).

Overall, the best results were obtained with UCX® plated at  $1.5 \times 10^4$  cells/cm<sup>2</sup> cell density on collagen coated plates, with 2% FBS at inoculation and further differentiation in 0% FBS, in the presence of Protocol C. Therefore this protocol was further adapted to 3D conditions.

### 3.2. UCX<sup>®</sup> differentiation into hepatocyte-like cells under 3D conditions

The 3D cell culture method in spheroids is a promising platform to achieve a more mature hepatocyte shape. Therefore, two protocols were adapted to 3D conditions: the *Reference Protocol*, which was chosen in order to test the 3D culture method and to be used as control; and the Protocol C, the differentiation protocol that presented the best results in 2D cultures. The 3D cultures consisted in spheroid cultured under static conditions, in ultra-low adherent 6-well plates.

In order to obtain aggregates with diameters within the range of 200-300  $\mu\text{m}$ , for the establishment of the hepatic differentiation under 3D conditions, the seeding density had to be optimized. Three seeding densities were tested ( $5 \times 10^4$ ,  $7.5 \times 10^4$  and  $1 \times 10^5$  cell/ $\text{cm}^2$ ) being  $7.5 \times 10^4$  cells/ $\text{cm}^2$  found to be best since it allowed the formation of spheroids with average sizes of  $115 \mu\text{m} \pm 48$  at day 2, and  $236 \pm 44 \mu\text{m}$  at day 24 (data not shown).

Regarding FBS concentration, although hepatocyte differentiation in 2D cultures is performed in serum free medium, the FBS presence is crucial for cells aggregation into spheroids in the 3D cultures. Thus, culture medium was supplemented with 10% FBS upon cells inoculation, and, once spheroids were formed, reduced to 2% FBS at day 2, since this was the minimum FBS concentration that allowed the maintenance of spheroid structure. The use of 0% FBS during the differentiation procedure was also attempted, but it resulted in disaggregation of cells (data not shown).

Therefore, for 3D cultures UCX<sup>®</sup> were inoculated at a concentration of  $7.5 \times 10^4$  cells/ $\text{cm}^2$  with culture medium supplemented with 10% FBS that was replaced by FBS free culture medium 1 day after cells inoculation.

#### 3.2.1 Characterization of the Differentiation Pattern of UCX<sup>®</sup> into hepatocyte-like cells (HLCs): *Reference Protocol* versus Protocol C

Many methods, commonly used to determine cell viability and metabolism, are incompatible with 3D systems. Thus, in order to assess the efficiency of UCX<sup>®</sup> differentiation in spheroids, namely cells viability, biochemical and metabolic

competence, samples were collected for H&E staining (viability evaluation), immunofluorescence (detection of the hepatic markers CK18, ALB and HNF4 $\alpha$ ), PAS staining (glycogen accumulation) and urea secretion (ammonia detoxification).

### **Cells Morphology within spheroids**

In both 3D differentiation protocols, UCX<sup>®</sup> formed spheroids with  $115 \pm 48 \mu\text{m}$  of diameter (mean  $\pm$  SD) after 2 days, reaching a diameter of  $236 \pm 44 \mu\text{m}$  (mean  $\pm$  SD) at the end of differentiation process, day 24 (Fig. 13).

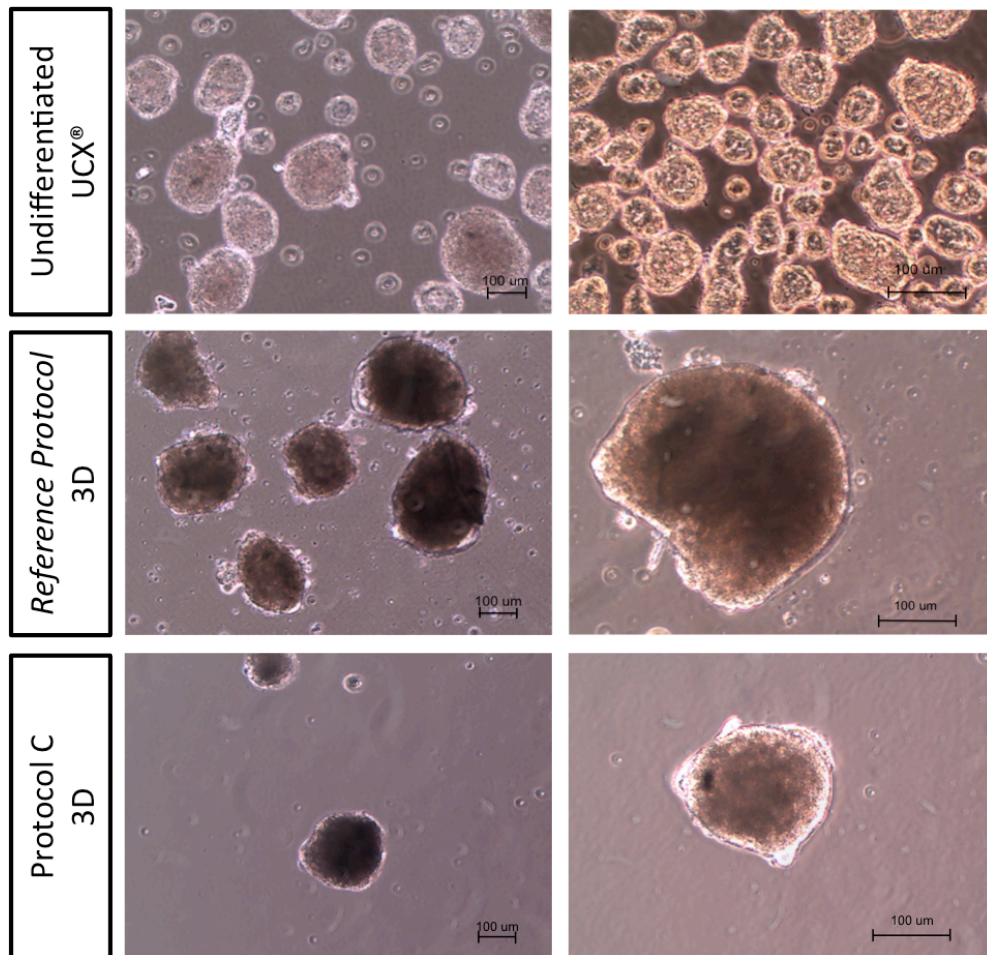


**Figure 13. Undifferentiated UCX<sup>®</sup> spheroids at day 2 and differentiated UCX<sup>®</sup> spheroids of *Reference Protocol* and *Protocol C* at day 24. Magnification: 10x (left), 20x (right).**

Cells within spheroids may have less access to nutrients and oxygen, thus the evaluation of cell viability under the optimized 3D culture conditions was critical. To assess the

viability of the cells within spheroids, cryosections of the spheroids were made and stained with the Hematoxylin-Eosin to detect the existence of necrotic centres. Hematoxylin-Eosin staining revealed the absence of necrotic centres, indicating that cells were viable in the interior of the spheroids (Figs. 14).

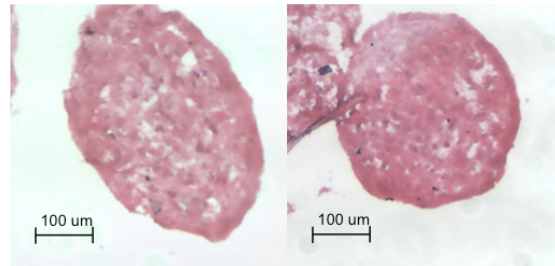


**Figure 14.** Hematoxylin-eosin staining of differentiated UCX® spheroids resultant from *Reference Protocol*. Magnification: 10x.

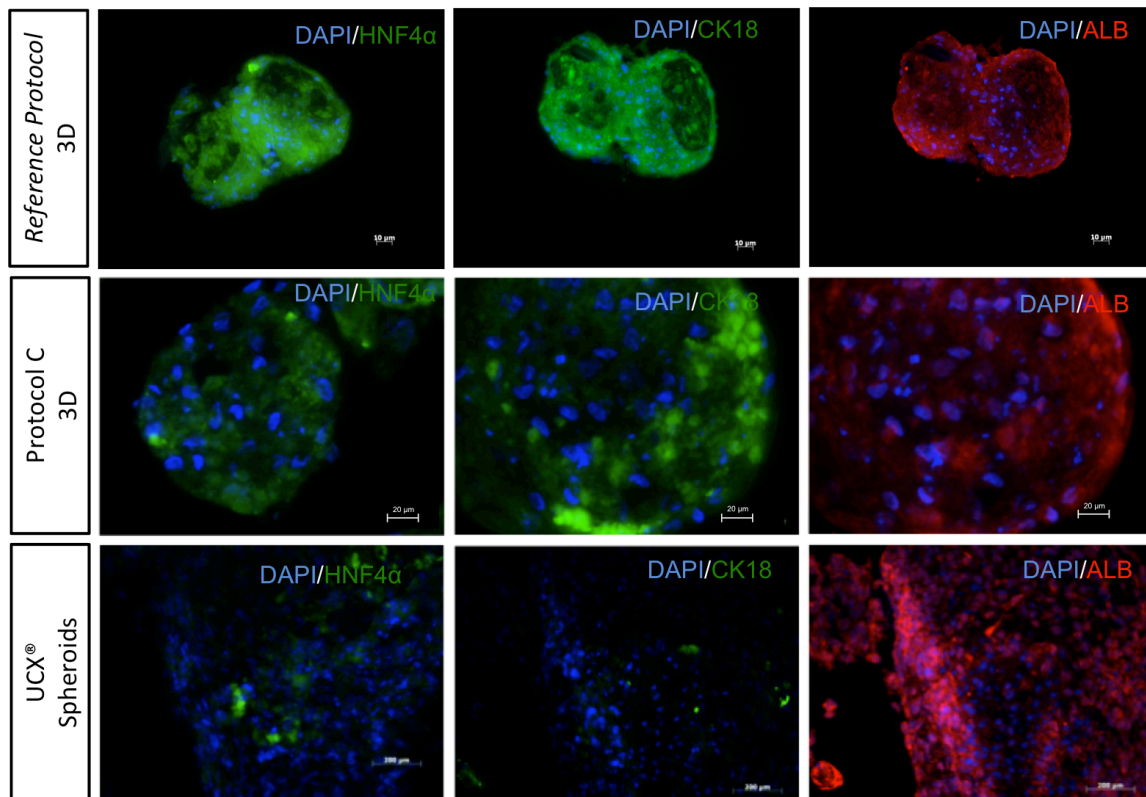


**Figure 15.** Presence of HNF4 $\alpha$ , ALB and CK18 in the differentiated UCX® at day 24 and in undifferentiated UCX®(negative control) in 3D culture method, detected by immunofluorescence staining. Magnification:40x (*Reference Protocol* 3D) 63x (Protocol C 3D and UCX® spheroids)



### **Characterization at the molecular level**

Immunofluorescence results revealed the presence of the hepatic markers CK18, ALB and HNF4 $\alpha$  in UCX<sup>®</sup> differentiated from both protocols in 3D cultures (Fig. 15). On the other hand, undifferentiated UCX<sup>®</sup> spheroids with 2 days accused the presence of ALB in the cytoplasm, which was not observed in 2D cell culture (Fig. 7).

### **Glycogen Storage**

At metabolic activity level, differentiated UCX<sup>®</sup> spheroids exposed to both protocols revealed glycogen accumulation in the cytoplasm as observed with PAS staining (Fig. 16). However, glycogen storage was also detected in undifferentiated UCX<sup>®</sup> spheroids. Indeed, high confluence of cells induce stem cells differentiation, which may explain the results obtained for PAS staining and albumin detection in immunofluorescence.

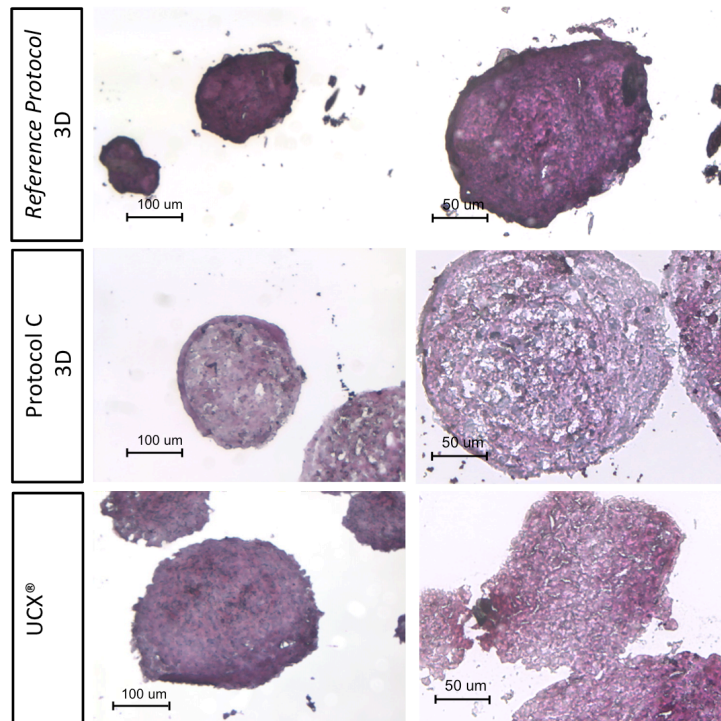


**Figure 16. Glycogen accumulation in differentiated UCX<sup>®</sup> at day 24 and undifferentiated UCX<sup>®</sup> in 3D culture method, determined by PAS staining. Magnification: 20x (left); 40x (right).**

### Urea production

Urea production was also tested in 3D cultures and compared to 2D differentiated UCX<sup>®</sup>. As in 2D differentiation, no urea production could be detected using the *Reference Protocol*. In contrast an increased 5-fold urea production was obtained when differentiating UCX<sup>®</sup> in 3D cultures with protocol C when compared to 2D differentiation (Fig. 17). These results, further suggest that hepatocyte differentiation may be improved when using 3D culture strategies.

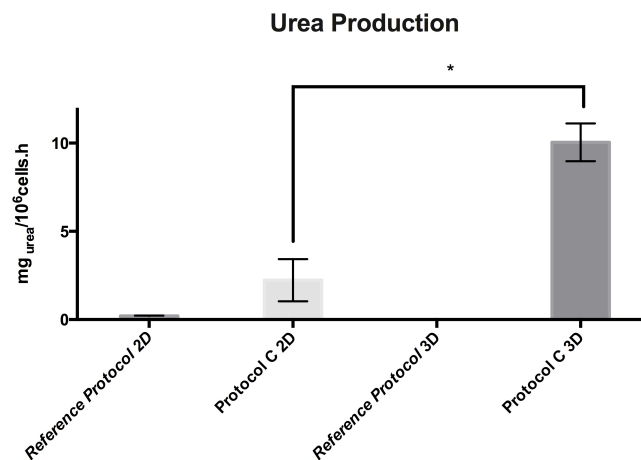


Figure 17. Urea production of differentiated UCX<sup>®</sup> of *Reference Protocol* and Protocol C in 2D and in 3D culture method at day 24. Data is represented as the mean  $\pm$  SD. \* $p < 0.05$ , \*\* $p < 0.01$ , \*\*\* $p < 0.001$ .

Overall, UCX<sup>®</sup> differentiated under 3D culture method showed hepatocyte-like cell characteristics. Differentiated UCX<sup>®</sup> showed the presence of the hepatic markers CK18, HNF4 $\alpha$ , and ALB detected by immunofluorescence in *Reference Protocol* and Protocol C. Moreover, glycogen accumulation was showed by PAS staining in differentiated UCX<sup>®</sup> exposed to both protocols. Finally, urea production could be improved when Protocol C was applied to 3D culture conditions.



## 4. Discussion

The main goal of this work was to develop a protocol capable of directing UCX® into hepatic fate, namely to produce differentiated HLCs with characteristics comparable to ratPHep, with the aim of using these cells as a platform for *in vitro* drug testing with closest similarity to human hepatocytes.

In order to optimize the differentiation protocol, a protocol described by Campard *et al* (2008)[25] was used as *Reference Protocol* to which alterations were made. The optimized protocol (Protocol C) was efficient in directing UCX® into HLC with the expression of hepatic markers ALB, CK18 and HNF4 $\alpha$  and the absence of the biliar marker CK19. These cells also showed glycogen storage capacity, activity of phase I (ECOD) and phase II (UGT) enzymes and urea production. The optimized protocol was implemented in 3D culture method and the results showed that this is a potential model to use in HLCs differentiation since in addition to maintaining the expression of hepatic markers tested (ALB, CK18 and HNF4 $\alpha$ ) this model allowed the increase in the urea production.

Modifications to *Reference Protocol* were made step-by-step under 2D conditions. The first parameter to be tested was FGF-2 concentration (Protocol A, see *Annex 1*) supported by embryogenesis studies [15]. During liver embryogenesis a FGF gradient is formed and is responsible for the segmentation of the endoderm. The lowest gradient of FGF induces the expression of *hhex*, a homeobox gene that regulates the hepatic genes, being hepatic fate repressed without its induction [15]. Moreover, Ameri *et al.* (2010)[38] determined the value of the concentration of FGF-2 ideal for directing definitive endoderm into foregut/midgut cell lineages, by testing different concentrations of FGF-2 (4 ng/mL, 16 ng/mL, 64 ng/mL and 256 ng/mL). It was found that the lower dose of FGF-2 (4 ng/mL) was the most effective in specifying hepatic fat.

In this work, two concentrations of FGF-2 were tested, 4 and 10 ng/mL. The obtained results showed that the lower concentration of FGF-2 was favourable to the expression of *hhex* gene resulting in the slight increase of metabolic activity of differentiated UCX<sup>®</sup> that was observed. Therefore, this concentration was implemented in all other optimization protocols.

The next step in the optimization of differentiation protocol was the addition of FGF-4 at the concentration of 10 ng/mL in step 2 (Protocol B, see Annex 1). This alteration was based in the hepatic differentiation protocols described in literature for adipose MSC, bmMSC and unrestricted somatic stem cells from umbilical cord blood [20, 58, 64]. For instance, Bonora-Centelles *et al.* (2009)[58] compared 3 different protocols for transdifferentiation of adipose MCS that included FGF-2 and EGF with FGF-4 or FGF-4 and BMP. The most effective protocol was the one with FGF-2 and EGF with FGF-4 at 10 ng/mL. Thus, these conditions were added to the step 2 of differentiation of the *Reference Protocol*, which was designated as Protocol B.

With the addition of FGF-4 and the lower concentration of FGF-2, *i.e.* 4 ng/mL, (Protocol B) the differentiated UCX<sup>®</sup>, besides the expression of CK18, HNF4 $\alpha$  and ALB hepatic markers, showed an improvement in urea production, ECOD and UGT activity.

The third alteration intended to increase the expression of liver-specific genes by directly targeting epigenetic mechanisms [42].

Epigenetics plays a very important role in cell differentiation. It is responsible for the silencing of pluripotent genes and activation of lineage-specific genes. The selection of expressed genes can be achieved by the alteration of the chromatin structure, which regulates the accessibility of transcription factors to gene promoters, meaning that the epigenetic code is responsible for the cell response to developmental signals during embryogenesis process [42].

The regulation and modification of chromatin structure is processed by specific enzymes, namely histone acetyl transferases (HATs), histone deacetylases (HDACs) and DNA methyltransferases (DNMTs). The first two enzymes are responsible for the acetylation

and deacetylation of lysine residues at the *N*-terminal histone tails. DNA accessibility to gene promoters is facilitated by histone acetylation since the acetylation weakens the link stability between DNA and histones. DNA methyltransferases (DNMT) catalyse the addition of a methyl group to the carbon-5 position of cytosine of CpG<sup>2</sup> islands present in gene promoters in DNA, therefore silencing gene expression [42].

It is described in literature the implication of HDAC and DNMT inhibitors in the upregulation of liver transcription factors [42]. Hence, the addition of HDAC and DNMT inhibitors in combination with growth factors is a promising protocol in directing UCX<sup>®</sup> into the hepatic fate. For this reason, an epigenetic modifier (DMSO) was included in Protocol C in order to test its influence in UCX<sup>®</sup> differentiation.

In recent studies, DMSO was shown to have effects in DNA methylation profiles. In mouse embryonic bodies, DMSO alters the DNA methylation profile, increasing the expression of *Dnmt3a*, which is a DNMT responsible for the *de novo* DNA methylation, therefore creating new methylation patterns [42, 65]. Though, recent findings show that *Dnmt1* and *Dnmt3b*, the first one responsible for the maintenance of DNA methylation patterns during DNA replication and the second one also responsible for new methylation, are inhibited by DMSO in osteoblast progenitor cells, MC3T3-E1 [42, 66]. In the same cells DMSO caused the increase of global DNA hydroxymethylation and the decrease of global DNA methylation. Yet, these effects are temporary and only affect cells methylation pattern during the first days of exposure to DMSO [66].

It was also reported that DMSO has effects in the maintenance of hepatocyte normal expression levels of liver transcription factors such as HNF4, C/EBP $\alpha$  and CYP (CYP2B1, CYP2B1, CYP3A1, CYP4A1) [67].

DMSO addition to differentiation protocol was based on the protocols of maturation of HepRG hepatoma cell line and fetal liver stem progenitor cells (FLSPC). These cells are in an undifferentiated state similar to hepatoblast state and in order to induce the maturation of these cells, they are exposed to 2% of DMSO (HepRG) or 1% DMSO (FLSPC) [9, 68].

---

<sup>2</sup> CpG islands are genomic regions rich in GC

Therefore, in Protocol C, 1% DMSO was added in the step 3 of differentiation, i.e., when cells are at the hepatoblast stage. The addition of 1% DMSO in the differentiation protocol resulted in a more homogenous and functionally active population of HLCs. CK18, ALB and HNF4 $\alpha$  were detected by immunofluorescence and qRT-PCR. Moreover, these cells seem to have reached a more mature phenotype, confirmed by the results of ECOD activity and urea production assays. Indeed, ECOD activity was higher in cells exposed to Protocol C than cells in the presence of *Reference Protocol*, Protocol A or B, as well as HepG2. In terms of UGT activity cells obtained with this protocol surpassed ratPHep metabolic activity.

Recently, 3D systems have been investigated and are considered good models for culturing cells *in vitro*. These systems mimic the *in vivo* environment, which can provide the cells with external clues important for restricting their multilineage potential, therefore causing them to differentiate, and maintaining this state for longer periods of time [22]. The 3D method chosen, cell spheroids, was previously demonstrated as an effective way of promoting functionality of primary hepatocytes [11, 30].

Thus, in this work, the *Reference Protocol* and Protocol C were established in 3D conditions. The protein expression levels of differentiated UCX<sup>®</sup>, such as ALB, CK18 and HNF4 $\alpha$ , were observed through immunostaining. Undifferentiated UCX<sup>®</sup> spheroid collected at day 2 of culture showed the presence of ALB and glycogen in the cytoplasm (Figs. 17 and 18). This, however, can be explained by the fact that high confluences of cells induce stem cell's differentiation [1].

Metabolic activity, in terms of glycogen storage and urea production was also significantly higher in 3D differentiated cells and even superior to the levels observed in ratPHep, demonstrating that the cell-to-cell contact and cell-ECM contact are important in the differentiation procedure [22]. These results suggest that the 3D culture method is a favourable method to direct ucmMSC into hepatic fate, therefore the development of this technique applied to the differentiation procedure is a promising approach.

## Conclusion

Overall, Protocol C combining FGF-2 concentration modification and addition of FGF-4 and DMSO provided a more homogenous functional population of human HLCs, with the expression of hepatocyte markers (ALB, CK18, HNF4 $\alpha$ ) and metabolic activity at a higher level than HepG2, the cell lineage most commonly used in toxicological assays. Regarding urea production, glycogen storage and UGT activity, the obtained HLCs achieved the activity levels of ratPHep. Moreover, the newly-tested 3D culture approach demonstrated potential in the differentiation of ucmMSCs into hepatic fate, with all the benefits of a cell spheroid culture.

The path towards functional and stable differentiated HLCs is still long. Growth factors and epigenetic modifiers should be explored and the 3D approach must be optimized. This includes exploiting other 3D cell culture methods, such as dynamic cultures in spinner flasks. If the differentiation turns out successful in terms of reproducibility and in obtaining an homogenous population of HLCs, this alternative source will be advantageous over other toxicity and metabolism models since these are expected to correctly mimic human liver processes.

## 5. Bibliography

1. Godoy P, Hewitt N, Albrecht U, Andersen M, Ansari N, Bhattacharya S, Bode J, Bolleyn J, Borner C, Böttger J *et al*: **Recent advances in 2D and 3D in vitro systems using primary hepatocytes, alternative hepatocyte sources and non-parenchymal liver cells and their use in investigating mechanisms of hepatotoxicity, cell signaling and ADME.** *Archives of toxicology* 2013, **87**(8):1315-1530.
2. Fox S: **Human Physiology** 12 edn. New York: McGraw Hill; 2011.
3. Anzenbacher P, Anzenbacherova E: **Enzyme systems of detoxication - overview of recent approaches.** *Interdisciplinary toxicology* 2008, **1**(1):6-7.
4. Guguen-Guillouzo C, Corlu A, Guillouzo A: **Stem cell-derived hepatocytes and their use in toxicology.** *Toxicology* 2010, **270**(1):3-9.
5. Buters J, Korzekwa K, Kunze K, Omata Y, Hardwick J, Gonzalez F: **cDNA-directed expression of human cytochrome P450 CYP3A4 using baculovirus.** *Drug metabolism and disposition: the biological fate of chemicals* 1994, **22**:688-692.
6. Kranendonk M, Mesquita P, Laires A, Vermeulen N, Rueff J: **Expression of human cytochrome P450 1A2 in Escherichia coli: a system for biotransformation and genotoxicity studies of chemical carcinogens.** *Mutagenesis* 1998, **13**(3):263-269.
7. Guillouzo A: **Liver Cell Models in in Vitro Toxicology.** *Environmental Health Perspectives* 1998, **106**:511-532.
8. Guguen-Guillouzo C: **Isolation and Culture of Animal and Human Hepatocytes.** In: *Culture of Epithelial Cells*. Edited by Freshney IF, M.G.; 2002.
9. Kanebratt K, Andersson T: **Evaluation of HepaRG cells as an in vitro model for human drug metabolism studies.** *Drug metabolism and disposition: the biological fate of chemicals* 2008, **36**(7):1444-1452.
10. Wilkening S, Stahl F, Bader A: **Comparison of primary human hepatocytes and hepatoma cell line HepG2 with regard to their biotransformation properties.** *Drug metabolism and disposition: the biological fate of chemicals* 2003, **31**(8):1035-1042.
11. Miranda J, Leite S, Muller-Vieira U, Rodrigues A, Carrondo M, Alves P: **Toward Extended Functional Hepatocyte In Vitro Culture.** *Tissue engineering Part C, Methods* 2009, **15**:1-11.
12. Boyer J, Graf J, Meier P: **Hepatic transport systems regulating pH<sub>i</sub>, cell volume, and bile secretion.** *Annual Review of Physiology* 1992, **54**:415-438.
13. O'Brien P, Chan K, Silber P: **Human and animal hepatocytes in vitro with extrapolation in vivo.** *Chemico-biological interactions* 2004, **150**(1):97-114.
14. Snykers S, Vanhaecke T, Papeleu P, Luttun A, Jiang Y, Vander Y, Verfaillie C, Rogiers V: **Sequential exposure to cytokines reflecting embryogenesis: the key for in vitro differentiation of adult bone marrow stem cells into functional hepatocyte-like cells.** *Toxicological sciences : an official journal of the Society of Toxicology* 2006, **94**(2):330-341.

15. Zorn AM: **Liver Development**. In: *StemBook [Internet]*. Cambridge(MA): harvard Stem Cell Institute; 2008.
16. Cai J, Zhao Y, Liu Y, Ye F, Song Z, Qin H, Meng S, Chen Y, Zhou R, Song X *et al*: **Directed differentiation of human embryonic stem cells into functional hepatic cells**. *Hepatology* 2007, **45**(5):1229-1239.
17. Hay D, Fletcher J, Payne C, Terrace J, Gallagher R, Snoeys J, Black J, Wojtacha D, Samuel K, Hannoun Z *et al*: **Highly efficient differentiation of hESCs to functional hepatic endoderm requires ActivinA and Wnt3a signaling**. *Proceedings of the National Academy of Sciences of the United States of America* 2008, **105**(34):12301-12306.
18. Agarwal S, Holton K, Lanza R: **Efficient differentiation of functional hepatocytes from human embryonic stem cells**. *Stem cells* 2008, **26**(5):1117-1127.
19. Duan Y, Ma X, Ma X, Zou W, Wang C, Bahbahan I, Ahuja T, Tolstikov V, Zern M: **Differentiation and characterization of metabolically functioning hepatocytes from human embryonic stem cells**. *Stem cells* 2010, **28**(4):674-686.
20. Snykers S, De Kock J, Tamara V, Rogiers V: **Hepatic differentiation of mesenchymal stem cells: in vitro strategies**. *Methods in molecular biology* 2011, **698**:305-314.
21. Piryaeei A, Valojerdi R, Shahsavani M, Baharvand H: **Differentiation of bone marrow-derived mesenchymal stem cells into hepatocyte-like cells on nanofibers and their transplantation into a carbon tetrachloride-induced liver fibrosis model**. *Stem cell reviews* 2011, **7**(1):103-118.
22. Okura M, Komoda H, Saga A, Yamamoto A, Hamada Y, Fumimoto Y, Lee CM, Ichinose A, Sawa Y, Matsuyama A: **Properties of Hepatocyte-like Cell Clusters from Human Adipose Tissue-Derived Mesenchymal Stem Cells**. *Tissue engineering Part C, Methods* 2010, **16**(4):761-770.
23. Sullivan G, Hay D, Park I-H, Fletcher J, Hannoun Z, Payne C, Dalgetty D, Black J, Ross J, Samuel K *et al*: **Generation of functional human hepatic endoderm from human induced pluripotent stem cells**. *Hepatology* 2010, **51**(1):329-335.
24. Si-Tayeb K, Noto F, Nagaoka M, Li J, Battle M, Duris C, North P, Dalton S, Duncan S: **Highly efficient generation of human hepatocyte-like cells from induced pluripotent stem cells**. *Hepatology* 2010, **51**(1):297-305.
25. Campard D, Lysy P, Najimi M, Sokal E: **Native umbilical cord matrix stem cells express hepatic markers and differentiate into hepatocyte-like cells**. *Gastroenterology* 2008, **134**(3):833-848.
26. Weiss M, Troyer D: **Stem cells in the umbilical cord**. *Stem cell reviews* 2006, **2**(2):155-162.
27. Anzalone R, Lo Iacono M, Corrao S, Magno F, Loria T, Cappello F, Zummo G, Farina F, La Rocca G: **New emerging potentials for human Wharton's jelly mesenchymal stem cells: immunological features and hepatocyte-like differentiative capacity**. *Stem cells and development* 2010, **19**(4):423-438.
28. Haycock J: **3D cell culture: a review of current approaches and techniques**. *Methods in molecular biology* 2011, **695**:1-15.

29. Tibbitt M, Anseth K: **Hydrogels as extracellular matrix mimics for 3D cell culture.** *Biotechnology and bioengineering* 2009, **103**(4):655-663.
30. Miranda J, Rodrigues A, Tostoes R, Leite S, Zimmerman H, Carrondo M, Alves P: **Extending hepatocyte functionality for drug-testing applications using high-viscosity alginate-encapsulated three-dimensional cultures in bioreactors.** *Tissue engineering Part C, Methods* 2010, **16**(6):1223-1232.
31. Baharvand H, Hashemi S, Kazemi S, Farrokhi A: **Differentiation of human embryonic stem cells into hepatocytes in 2D and 3D culture systems in vitro.** *The International journal of developmental biology* 2006, **50**(7):645-652.
32. Wilson C, Clegg R, Leavesley D, Pearcy M: **Mediation of biomaterial-cell interactions by adsorbed proteins: a review.** *Tissue Engineering* 2005, **11**(1-2):1-18.
33. Shen M: **Nodal signaling: developmental roles and regulation.** *Development* 2007, **134**(6):1023-1034.
34. Calmont A, Wandzioch E, Tremblay K, Minowada G, Kaestner K, Martin G, Zaret K: **An FGF response pathway that mediates hepatic gene induction in embryonic endoderm cells.** *Developmental cell* 2006, **11**(3):339-348.
35. McLin V, Rankin S, Zorn A: **Repression of Wnt/beta-catenin signaling in the anterior endoderm is essential for liver and pancreas development.** *Development* 2007, **134**(12):2207-2217.
36. Chen Y, Pan F, Brandes N, Afelik S, Sölter M, Pieler T: **Retinoic acid signaling is essential for pancreas development and promotes endocrine at the expense of exocrine cell differentiation in *Xenopus*.** *Developmental biology* 2004, **271**(1):144-160.
37. Zaret K: **Liver specification and early morphogenesis.** *Mechanisms of Development* 2000, **92**:83-88.
38. Ameri J, Stahlberg A, Pedersen J, Johansson J, Johannesson M, Artner I, Semb H: **FGF2 specifies hESC-derived definitive endoderm into foregut/midgut cell lineages in a concentration-dependent manner.** *Stem cells* 2010, **28**(1):45-56.
39. Rossi J, Dunn N, Hogan B, Zaret K: **Distinct mesodermal signals, including BMPs from the septum transversum mesenchyme, are required in combination for hepatogenesis from the endoderm.** *Gene development* 2001, **15**(15):1998-2009.
40. Bort R, Signore M, Tremblay K, Martinez Barbera J, Zaret K: **Hex homeobox gene controls the transition of the endoderm to a pseudostratified, cell emergent epithelium for liver bud development.** *Developmental biology* 2006, **290**(1):44-56.
41. Wang Z, Dollé P, Cardoso W, Niederreither K: **Retinoic acid regulates morphogenesis and patterning of posterior foregut derivatives.** *Developmental biology* 2006, **297**(2):433-445.
42. Snykers S, De Kock J, Rogiers V, Vanhaecke T: **In vitro differentiation of embryonic and adult stem cells into hepatocytes: state of the art.** *Stem cells* 2009, **27**(3):577-605.



43. Kamiya AK, T.; Miyajima, A. : **Oncostatin M and Hepatocyte Growth Factor Induce Hepatic Maturation Via Distinct Signaling Pathways.** *FEBS Letters* 2001(492):90-94.
44. Kamiya A, Kinoshita T, Ito Y, Matsui T, Morikawa Y, Senba E, Nakashima K, Taga T, Yoshida K, Kishimoto T *et al*: **Fetal liver development requires a paracrine action of Oncostatin M through the gp130 signal transducer.** *The EMBO Journal* 1999, **18**(8):2127-2136.
45. Odom D, Zizlsperger N, Gordon D, Bell GW, Rinaldi N, Murray H, Volkert T, Schreiber J, Rolfe P, Gifford D *et al*: **Control of pancreas and liver gene expression by HNF transcription factors.** *Science* 2004, **303**(5662):1378-1381.
46. Michalopoulos GB, W.; Mulé,K.; Luo, J.: **HGF,EGF and Dexamethasone induced gene expression patterns during formation of tissue in hepatic organoid cultures.** *Gene Expression* 2003, **11**(2):55-75.
47. D'Amour K, Agulnick A, Eliazar S, Kelly O, Kroon E, Baetge E: **Efficient differentiation of human embryonic stem cells to definitive endoderm.** *Nature biotechnology* 2005, **23**(12):1534-1541.
48. Brolén G, Sivertsson L, Björquist P, Eriksson G, Ek M, Semb H, Johansson I, Andersson T, Ingelman-Sundberg M, Heins N: **Hepatocyte-like cells derived from human embryonic stem cells specifically via definitive endoderm and a progenitor stage.** *Journal of biotechnology* 2010, **145**(3):284-294.
49. Lefort N, Feyeux M, Bas C, Feraud O, Bennaceur-Griscelli A, Tachdjian G, Peschanski M, Perrier AL: **Human embryonic stem cells reveal recurrent genomic instability at 20q11.21.** *Nature biotechnology* 2008, **26**(12):1364-1366.
50. Duret C, Gerbal-Chaloin S, Ramos J, Fabre J, Jacquet E, Navarro F, Blanc P, Sa-Cunha A, Maurel P, Daujat-Chavanieu M: **Isolation, characterization, and differentiation to hepatocyte-like cells of nonparenchymal epithelial cells from adult human liver.** *Stem cells* 2007, **25**(7):1779-1790.
51. Takahashi K, Yamanaka S: **Induction of pluripotent stem cells from mouse embryonic and adult fibroblast cultures by defined factors.** *Cell* 2006, **126**(4):663-676.
52. Takahashi K, Tanabe K, Ohnuki M, Narita M, Ichisaka T, Tomoda K, Yamanaka S: **Induction of pluripotent stem cells from adult human fibroblasts by defined factors.** *Cell* 2007, **131**(5):861-872.
53. Song Z, Cai J, Liu Y, Zhao D, Yong J, Duo S, Song X, Guo Y, Zhao Y, Qin H *et al*: **Efficient generation of hepatocyte-like cells from human induced pluripotent stem cells.** *Cell research* 2009, **19**(11):1233-1242.
54. O'Donoghue K, Fisk N: **Fetal stem cells.** *Best Practice & Research Clinical Obstetrics and gynaecology* 2004, **18**(6):853-875.
55. Salem H, Thiemermann C: **Mesenchymal stromal cells: current understanding and clinical status.** *Stem cells* 2010, **28**(3):585-596.
56. Dominici M, Le Blanc K, Mueller I, Slaper-Cortenbach I, Marini F, Krause D, Deans R, Keating A, Prockop D, Horwitz E: **Minimal criteria for defining multipotent mesenchymal stromal cells. The International Society for Cellular Therapy position statement.** *Cytotherapy* 2006, **8**(4):315-317.

57. Banas A, Teratani T, Yamamoto Y, Tokuhara M, Takeshita F, Osaki M, Kato T, Okochi H, Ochiya T: **Rapid hepatic fate specification of adipose-derived stem cells and their therapeutic potential for liver failure.** *Journal of gastroenterology and hepatology* 2009, **24**(1):70-77.
58. Bonora-Centelles A, Jover R, Mirabet V, Lahoz A, Carbonell F, Castell J, Gómez-Lechón M: **Sequential hepatogenic transdifferentiation of adipose tissue-derived stem cells: relevance of different extracellular signaling molecules, transcription factors involved, and expression of new key marker genes.** *Cell Transplant* 2009, **18**(12):1319-1340.
59. Santos J, Bárcia R, Simões S, Gaspar M, Calado S, Agua-Doce A, Almeida S, Almeida J, Filipe M, Teixeira M *et al*: **The role of human umbilical cord tissue-derived mesenchymal stromal cells (UCX®) in the treatment of inflammatory arthritis.** *Journal of translational medicine* 2013, **11**:18.
60. Troyer D, Weiss M: **Wharton's jelly-derived cells are a primitive stromal cell population.** *Stem cells* 2008, **26**(3):591-599.
61. Schwartz RE, Reyes M, Koodie L, Jiang Y, Blackstad M, Lund T, Lenvik T, Johnson S, Hu W-S, Verfaillie CM: **Multipotent adult progenitor cells from bone marrow differentiate into functional hepatocyte-like cells.** *Journal of Clinical Investigation* 2002, **109**(10):1291-1302.
62. Chen M-L: **HNF-4 $\alpha$  determines hepatic differentiation of human mesenchymal stem cells from bone marrow.** *World Journal of Gastroenterology* 2010, **16**:5092-5103.
63. Gómez-Lechón M, Lahoz A, Castell J, Donato M: **Evaluation of cytochrome P450 activities in human hepatocytes in vitro.** *Methods in molecular biology* 2012, **806**:87-97.
64. Waclawczyk S, Buchheiser A, Flogel U, Radke F, Kogler G: **In vitro differentiation of unrestricted somatic stem cells into functional hepatic-like cells displaying a hepatocyte-like glucose metabolism.** *Journal of cellular physiology* 2010, **225**(2):545-554.
65. Iwatani M, Ikegami K, Kremenska Y, Hattori N, Tanaka S, Yagi S, Shiota K: **Dimethyl sulfoxide has an impact on epigenetic profile in mouse embryoid body.** *Stem cells* 2006, **24**(11):2549-2556.
66. Thaler R, Spitzer S, Karlic H, Klaushofer K, Varga F: **DMSO is a strong inducer of DNA hydroxymethylation in pre-osteoblastic MC3T3-E1 cells.** *Epigenetics* 2012, **7**(6):635-651.
67. Su T, Waxman D: **Impact of dimethyl sulfoxide on expression of nuclear receptors and drug-inducible cytochromes P450 in primary rat hepatocytes.** *Archives Biochemistry and Biophysics* 2004, **424**(2):226-234.
68. Liu W, Liu Z, You N, Zhang N, Wang T, Gong Z, Liu H, Dou K: **Several important in vitro improvements in the amplification, differentiation and tracing of fetal liver stem/progenitor cells.** *PloS one* 2012, **7**(10):1-9.

## Annex 1- Hepatic differentiation protocols

Liver embryogenesis stage	<i>In vitro</i> step	<i>Reference Protocol</i> and 2D optimization
Induction of Hepatic Competence	Step1	EGF (20ng/mL) FGF2 (10ng/mL) <b>FGF2 (4ng/mL):Protocol A</b>
Hepatoblast and liver bud formation	Step 2	FGF2 (10ng/mL) HGF (20ng/mL) ITS (1%) Nicotinamide (0,61g/L) <b>FGF4 (10ng/mL): Protocol B</b>
Maturation into Hepatocyte	Step 2	Dexa (1umol/L) OSM (20ng/mL) ITS (1%) <b>DMSO(1%): Protocol C</b>

## Annex 2- Primers used in qRT-PCR

Gene	Primer Forward	Primer Reverse	Reference
<i>hhex</i>	GCTTCAGAACCCATCCATGT	TTCCCCTCACGAAGAAGTTG	[38]
<i>ck18</i>	TGGTACTCTCCTCAATCTGCTG	CTCTGGATTGACTGTGGAAGT	[61]
<i>ck19</i>	ATGGCCGAGCAGAACCGGAA	CCATGAGCCGCTGGTACTCC	[61]
<i>alb</i>	TGCTTGAATGTGCTGATGACAGGG	AAGGCAAGTCAGCAGGCATCTCATC	[62]
<i>gapdh</i>	GAAGGTGAAGGTCGGAG	GAAGATGGTGATGGGATTTTC	[38]